New Phytologist

Research

An inosine triphosphate pyrophosphatase safeguards plant nucleic acids from aberrant purine nucleotides

Henryk Straube[1], Jannis Straube[2], Jannis Rinne[1], Lisa Fischer[1], Markus Niehaus[1], Claus-Peter Witte[1] and Marco Herde[1]

[1]Department of Molecular Nutrition and Biochemistry of Plants, Leibniz Universität Hannover, Hannover 30419, Germany; [2]Department of Molecular Plant Breeding, Leibniz Universität Hannover, Hannover 30419, Germany

Author for correspondence:
Marco Herde
Email: mherde@pflern.uni-hannover.de

Received: *20 May 2022*
Accepted: *22 November 2022*

New Phytologist (2023) **237:** 1759–1775
doi: 10.1111/nph.18656

Key words: abiotic stress, damaged metabolites, deaminated purine nucleotides, inosine triphosphate, inosine triphosphate pyrophosphatase, plant nucleotide metabolism, senescence.

Summary

- In plants, inosine is enzymatically introduced in some tRNAs, but not in other RNAs or DNA. Nonetheless, our data show that RNA and DNA from *Arabidopsis thaliana* contain (deoxy)inosine, probably derived from nonenzymatic adenosine deamination in nucleic acids and usage of (deoxy)inosine triphosphate (dITP and ITP) during nucleic acid synthesis.
- We combined biochemical approaches, LC–MS, as well as RNA-Seq to characterize a plant INOSINE TRIPHOSPHATE PYROPHOSPHATASE (ITPA) from *A. thaliana*, which is conserved in many organisms, and investigated the sources of deaminated purine nucleotides in plants.
- Inosine triphosphate pyrophosphatase dephosphorylates deaminated nucleoside di- and triphosphates to the respective monophosphates. *ITPA* loss-of-function causes inosine di- and triphosphate accumulation *in vivo* and an elevated inosine and deoxyinosine content in RNA and DNA, respectively, as well as salicylic acid (SA) accumulation, early senescence, and upregulation of transcripts associated with immunity and senescence. Cadmium-induced oxidative stress and biochemical inhibition of the INOSINE MONOPHOSPHATE DEHYDROGENASE leads to more IDP and ITP in the wild-type (WT), and this effect is enhanced in *itpa* mutants, suggesting that ITP originates from ATP deamination and IMP phosphorylation.
- Inosine triphosphate pyrophosphatase is part of a molecular protection system in plants, preventing the accumulation of (d)ITP and its usage for nucleic acid synthesis.

Introduction

Spontaneous or enzymatically catalyzed reactions can lead to damaged or aberrant metabolites (Linster *et al.*, 2013; Lerma-Ortiz *et al.*, 2016; Crécy-Lagard *et al.*, 2018). In recent years, several advances have been made in the field of damaged plant metabolites (Hanson *et al.*, 2016), like the discovery of enzymes repairing NAD(P)H hydrates (Niehaus *et al.*, 2014), removing damaged glutathione (Niehaus *et al.*, 2019) and oxidized deoxyguanosine triphosphate (8-oxo dGTP; Dobrzanska *et al.*, 2002; Yoshimura *et al.*, 2007). One of the most prominent metabolite classes that are prone to become damaged are nucleotides (Galperin *et al.*, 2006; Rampazzo *et al.*, 2010; Nagy *et al.*, 2014; Rudd *et al.*, 2016). In nonplant organisms, several enzymes have been identified that repair or remove aberrant and often toxic nucleotides, like DEOXYURIDINE TRIPHOSPHATE PYROPHOSPHATASE (DUT1), INOSINE TRIPHOSPHATE PYROPHOSPHATASE (ITPA), 8-OXO DEOXYGUANOSINE TRIPHOSPHATE PYROPHOSPHATASE (NUDX1), and MULTICOPY-ASSOCIATED FILAMENTATION (MAF) family proteins (Nagy *et al.*, 2014). However, little is known about such enzymes in plants. While plant homologues of DUT1 and NUDX1 (Yoshimura *et al.*, 2007; Dubois *et al.*, 2011) have been characterized, a plant ITPA has not been described.

Inosine triphosphate pyrophosphatase (ITPA) enzymes from *Escherichia coli* and *Homo sapiens* remove deaminated purine nucleotide triphosphates. They exclusively hydrolyze the phosphoanhydride bond between the alpha- and beta-phosphate of (deoxy)inosine triphosphate (ITP and dITP) probably derived from the deamination of (deoxy)adenosine triphosphate (ATP and dATP) or from spurious phosphorylation of inosine monophosphate (IMP). Xanthosine triphosphate (XTP), presumably derived from the deamination of guanosine triphosphate (GTP) or spurious phosphorylation of xanthosine monophosphate (XMP), is also a substrate (Lin *et al.*, 2001; Davies *et al.*, 2012). Inosine triphosphate pyrophosphatase generates the corresponding nucleotide monophosphate and pyrophosphate. Whereas (d)ITP and XTP are aberrant nucleotides, IMP and XMP are canonical intermediates of guanosine monophosphate (GMP) synthesis in most organisms and in plants XMP is additionally a starting point of purine nucleotide catabolism (Heinemann *et al.*, 2021).

Deamination of cytosine to uracil is well known to occur in nucleic acids (Lindahl & Nyberg, 1974; Frederico *et al.*, 1990), but purine bases can also be deaminated. *In vitro*, the deamination of adenine to hypoxanthine in DNA occurs at 2% to 3% of

the rate observed for cytosine to uridine conversion (Lindahl, 1993). The deamination of free nucleotides is less well documented. Purine deamination was shown to occur not only in the nucleic acids but also in the pool of free nucleotides under heat stress (Karren & Lindahl, 1980). In general abiotic stresses, like salinity, water stress, extreme temperature, wounding, UV radiation, or exposure to heavy metals (Valderrama *et al.*, 2007; Corpas *et al.*, 2011) may influence the rate of nucleotide deamination. These stresses generate reactive nitrogen or oxygen species (RNS, ROS; Valderrama *et al.*, 2007; Corpas *et al.*, 2011), which are mainly discussed in the context of protein modification and lipid peroxidation but are also likely damaging other metabolites although this has rarely been shown so far (Demidchik, 2015).

Inosine triphosphate and dITP are substrates of RNA and DNA polymerases, respectively. Random inosine or deoxyinosine in nucleic acids can thus not only be derived from the deamination of adenosine or deoxyadenosine in the polymer but may also be incorporated during polymerization. When DNA, containing deaminated sites, is replicated, mutations may be introduced. Deoxycytidine can be incorporated opposite of deoxyinosine and often thymidine is placed opposite of deoxyxanthosine (Kamiya, 2003). This misincorporation is not directly detrimental for *E. coli* (Budke & Kuzminov, 2006) because it is rapidly repaired. However, upon stimulation of deamination, the constant deployment of the repair machinery leads to strand breaks and chromosomal rearrangements (Budke & Kuzminov, 2010). By contrast, deoxyinosine in human DNA causes mutations and genome instability even when deamination is not stimulated (Yoneshima *et al.*, 2016; DeVito *et al.*, 2017). During RNA synthesis in nonplant organisms, incorporation of ITP has been shown to significantly reduce transcriptional velocity. Inosine in RNA alters RNA structure and stability and leads to mistranslation (Thomas *et al.*, 1998; Ji *et al.*, 2017) or stalling of translation (Schroader *et al.*, 2022). Apart from effects on nucleic acids, ITP and XTP can interfere with various ATP- and GTP-dependent cellular processes (Osheroff *et al.*, 1983; Carnelli *et al.*, 1992; Klinker & Seifert, 1997; Muraoka *et al.*, 1999; Weber & Senior, 2001).

Inosine triphosphate has been detected *in vivo* in only a few occasions. Human erythrocytes accumulated radioactive ITP after incubation with [^{14}C] adenine, [^{14}C] guanine, or [^{14}C] hypoxanthine, indicating that a biosynthetic route to deaminated purine nucleotide triphosphates might exist (Fraser *et al.*, 1975). Interestingly, a loss of ITPA function in erythrocytes of mice leads to a substantial accumulation of ITP of up to 10% to 25% of the ATP pool (Behmanesh *et al.*, 2009). However, erythrocytes are a special cell type, which lack nuclear DNA and seem to have a particular nucleotide metabolism. It is technically challenging to detect ITP and XTP at all. In human cancer cells, both were detected with a highly sensitive method in the fmol mg^{-1} protein range. Here, ITP was around 5–10 times more abundant than XTP (Jiang *et al.*, 2018). To date, the corresponding deoxyribonucleotide triphosphates, dITP and deoxyxanthosine triphosphate (dXTP), have never been detected in any organism.

Although these metabolites are low abundant, they can be incorporated into nucleic acids. The frequency of inosine in RNA is about one in 10^5 nucleosides in wild-type (WT) *E. coli*, while deoxyinosine in DNA is 10-fold less abundant (Pang *et al.*, 2012). In mutants of rdgB, the bacterial ITPA homolog, the inosine content of RNA increased *c.* 10-fold and the deoxyinosine of DNA rose about fivefold compared with the WT (Pang *et al.*, 2012). In *ITPA* knockout mice, the inosine-to-adenosine ratio was about one per 100 nucleosides in RNA (Behmanesh *et al.*, 2009). In mammals, ITPA deficiency causes drastic phenotypes. In humans, it leads to a lethal Martsolf-like syndrome with neurological and developmental abnormalities (Handley *et al.*, 2019). Mice without a functional ITPA had RNA with an elevated inosine content and died shortly after birth (Behmanesh *et al.*, 2009). However, bacteria lacking ITPA are viable (Burgis *et al.*, 2003). Recently, a homolog of ITPA in *Cassava brown streak virus*, a plant-infecting RNA virus, was demonstrated to be an important factor during viral infection (Tomlinson *et al.*, 2019), interacting with the viral RNA-dependent RNA polymerase (Valli *et al.*, 2022).

In this study, we identified ITPA of *A. thaliana* and biochemically characterized the enzyme, showing that it catalyzes the dephosphorylation of deaminated purine nucleotides. We analyzed mutants of *ITPA* demonstrating that the enzyme safeguards nucleic acids from incorporation of (d)ITP. We were able to detect ITP and IDP accumulation in the mutants and investigated the metabolic source of ITP and IDP. In contrast to *itpa* mutants in mammals, the Arabidopsis mutants have only minor phenotypic alterations. They show slightly earlier senescence and have elevated concentrations of the defense phytohormone salicylic acid (SA), triggering a transcriptional response of genes associated with SA, systemic acquired resistance (SAR) and aging.

Materials and Methods

Plant cultivation

Arabidopsis thaliana (L.) Heynh and *Nicotiana benthamiana* plants were cultivated as described recently (Witte *et al.*, 2005; Straube *et al.*, 2021).

A segregating T-DNA insertion line from the SALK collection (*itpa*-1, SALK_052023; Alonso *et al.*, 2003) was acquired from the Nottingham Arabidopsis Stock Centre. A homozygous knockout line and a corresponding WT were selected from the segregating population (see Methods S1).

A second knockout line was obtained via genome editing (*itpa*-2) according to Rinne *et al.* (2021; see Methods S1). A line overexpressing ITPA (*itpa-2::C*) was generated (see Methods S1).

For root-length and germination assays, plants were grown in Petri dishes on previously described medium (Niehaus *et al.*, 2020; Straube *et al.*, 2021).

Plants for the cadmium sulfate feeding experiment were grown hydroponically according to Batista-Silva *et al.* (2019), with small modifications. Plants were grown in viscous liquid medium (Niehaus *et al.*, 2020; Straube *et al.*, 2021) containing 0.4% agar under long-day conditions. Cadmium treatment was performed for 24 h by adding a 500 mM cadmium sulfate solution to a final concentration of 10 μM to the medium, respectively. This concentration was chosen according to Di Sanità & Gabbrielli (1999).

DNA extraction, RNA extraction, genotyping, qRT-PCR, and cloning

DNA for genotyping was isolated according to the BOMB protocol using the TNA extraction from plants with the TNES/GITC lysis protocol (Oberacker *et al.*, 2019). Magnetic beads were silica-coated beads, synthesized using the BOMB protocol for coating ferrite magnetic nanoparticles with silica oxide (Oberacker *et al.*, 2019).

Total RNA was isolated using the Plant NucleoSpin II kit (Macherey-Nagel, Düren, Germany) according to the manufacturer's specifications.

For information on genotyping, qRT-PCR, and cloning, see Methods S1. Primers used in this study are provided in Table S1.

Protein purification, quantification, and enzymatic assay

C-terminal strep-tagged ITPA, AMPK3, and AMPK4 (Chen *et al.*, 2018) were transiently overexpressed in *N. benthamiana* and affinity purified after 5 d as described previously (Werner *et al.*, 2008). The protein concentration was determined by an in-gel quantification assay using a Li-Cor Odyssey FC with Image Studio software. SDS gel electrophoresis and staining were performed as described previously (Witte *et al.*, 2005).

Enzymatic assays for ITPA were performed using the EnzChek™ Pyrophosphate Assay Kit (ThermoFisher Scientific, Waltham, MA, USA) according to the manufacturer's instructions, with the exception of reducing the volume of all solution to one-fifth of the instructions using High Precision Cells (Hellma Analytics, Müllheim, Germany).

AMPK3 and 4 activity was determined using a coupled enzyme assay with pyruvate kinase and lactate dehydrogenase (LDH, P0294; Sigma-Aldrich, St Louis, MO, USA), measuring the production of NAD^+ that results in absorption decrease at 340 nm. For details, see Methods S1.

Subcellular localization

A construct encoding ITPA fused to C-terminal YELLOW FLUORESCENT PROTEIN (YFP) was transiently coexpressed in *N. benthamiana* with a construct encoding cytosolic β-ureidopropionase C-terminally fused to CYAN FLUORESCENT PROTEIN (CFP). Whole leaves were immersed in octadecafluordecahydronaphthalin (Sigma-Aldrich; Littlejohn *et al.*, 2010). The samples were analyzed using a Leica True Confocal Scanner SP8 microscope equipped with an HC PL APO CS2 40 × 1.10 water immersion objective (Leica, Wetzlar, Germany) as described in Dahncke & Witte (2013). The acquired images were processed using Leica Application Suite Advanced Fluorescence software (Leica Microsystems, Wetzlar, Germany). The immunoblot to analyze the construct was developed using a GREEN FLUORESCENT PROTEIN (GFP)-specific antibody. Co-localization was analyzed using the JACoP-plugin in ImageJ (Bolte & Cordelieres, 2006).

Metabolite analysis

The analysis of nucleotide concentration was performed as recently described with slight modifications (Straube *et al.*, 2021; Straube & Herde, 2022). For details, see Methods S1.

Salicylic acid (SA) was extracted and measured according to Cao *et al.* (2014) and Yang *et al.* (2017).

Quantitative determination of (deoxy)inosine per (deoxy) adenosine level in total RNA and DNA

DNA was extracted using a modified CTAB- (hexadecyltrimethylammonium bromide) based protocol (see Methods S1). Total RNA was isolated using the Plant NucleoSpin II kit (Macherey-Nagel) according to the manufacturer's specifications.

Nucleic acids were digested using the Nucleoside Digestion Mix (New England Biolabs, Ipswich, MA, USA) with the following modifications: 5 µl Nucleoside Digestion Mix Reaction Buffer (10×) and 0.5 µl Nucleoside Digestion Mix were used, adding RNA or DNA and water depending on the respective concentration of the RNA or DNA up to a total volume of 50 µl. The mixture was incubated for 4 h at 37°C. A total of 1 µg RNA or 3 µg DNA was digested.

Digested RNA and DNA was measured by HPLC–MS as recently published (Traube *et al.*, 2019), with minor modifications (Methods S1).

Analysis of chlorophyll content

Measurement of chlorophyll content was performed as described previously (Harris & Baulcombe, 2015).

Cell death staining and quantification

Trypan blue staining was performed as published recently (Fernández-Bautista *et al.*, 2016). To quantify the leaf area affected by cell death, RGB pictures of stained leaves were taken and stained cell areas were quantified using ImageJ.

Sequence analysis and phylogenetic analysis

Inosine triphosphate pyrophosphatases sequences were identified using the Phytozome v.12.1 webserver (https://phytozome.jgi.doe.gov/pz/portal.html) and the National Center for Biotechnology (NCBI) for all nonplant organisms employing Blastp searches with the *Arabidopsis* amino acid sequence. The alignment and phylogenetic tree were constructed as described recently (Heinemann *et al.*, 2021). The alignment used to construct the phylogenetic tree is shown in Fig. S1. For details, see Methods S1.

RNA-seq analysis

Total RNA from 35-d-old rosette leaves from *A. thaliana* Col-0 ('wild type') and *itpa*-1 plants was sent for Illumina mRNA

sequencing to Novogene (Cambridge, UK). For details, see Methods S1.

Ribavirin treatment

Arabidopsis thaliana and *N. benthamiana* plants were either mock-treated or with buffer containing ribavirin, an inhibitor of the IMP DEHYDROGENASE. For details, see Methods S1.

Statistical analysis

Statistical analysis was performed as stated in Heinemann *et al.* (2021). The number of replicates, test values, and multiplicity-adjusted *P*-values are reported in Table S4.

Results

Comprehensive phylogenetic analysis of inosine triphosphate pyrophosphatase in plants

We used the amino acid sequence of human ITPA to search with BLASTP for homologs in plants (Fig. S2). For *A. thaliana*, the protein encoded at the gene locus At4g13720 was the only candidate with a high sequence similarity to the human ITPA. It has been suggested previously that this enzyme may represent a plant ITPA (Lin *et al.*, 2001; James *et al.*, 2021). A phylogenetic analysis revealed that ITPA is present in all kingdoms of life including plants and algae (Figs 1, S1).

Several amino acid residues are highly conserved in ITPAs from different species. Many of these have been shown to be relevant for substrate binding, catalytic activity, and dimerization (Figs S1, S2; Savchenko *et al.*, 2007; Stenmark *et al.*, 2007; Gall *et al.*, 2013). Nonetheless, there are amino acid residues that are only conserved in plant ITPAs (Figs S1, S2). Among these, K/R 183 and K/R 189 can be acetylated in Arabidopsis (Liu *et al.*, 2018), but the function of these posttranslational modifications is unclear.

ITPA has atypical characteristics for an ITP pyrophosphatase

Inosine triphosphate pyrophosphatases are described in other organisms to hydrolyze the phosphoanhydride bond between the alpha- and beta-phosphate groups of inosine triphosphate resulting in IMP and pyrophosphate (Fig. 2a).

To assess the activity of the plant enzyme, a C-terminal Strep-tagged variant of ITPA was transiently expressed in *N. benthamiana* and affinity purified (Fig. 2b). Interestingly, two forms of the protein were purified represented by two bands in a Coomassie-stained SDS-PAGE, possibly indicating a posttranslational modification. The identity of the purified protein was confirmed by immunoblot with an antibody against the Strep-tag. The specific activity of the purified enzyme was determined with several substrates at concentrations of 200 µM, including (deoxy)ribonucleotide di-, and triphosphates, *para*-nitrophenyl-phosphate and nicotinamide adenine dinucleotide (Fig. 2c; Table S5). An enzymatic activity could only be observed with dITP, ITP, inosine

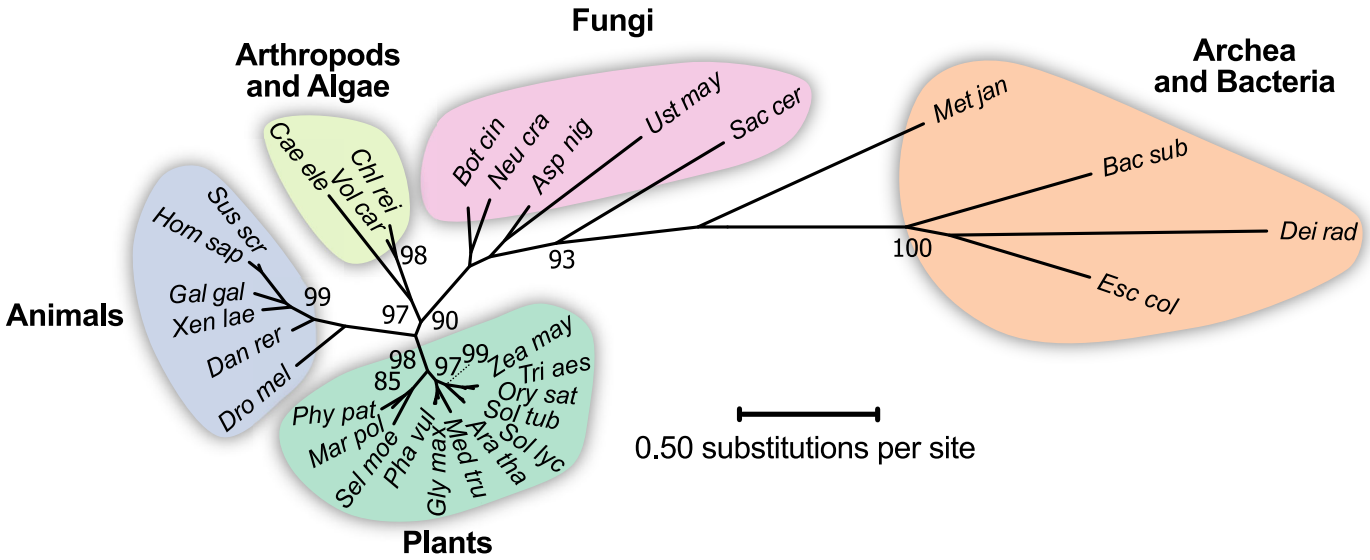

Fig. 1 Phylogenetic analysis of ITPA in several organisms. An unrooted maximum likelihood tree was built using MEGAX, comprising model species from a wide taxonomic range. The tree with the best log score is shown with branch length indicating the number of site substitutions (scale bar). Numbers at branches indicate the percentage of trees in which associated taxa clustered together in the bootstrap analysis (1000 bootstraps). Values below 80 are not shown. Species names are abbreviated as follows: Asp nig, *Aspergillus niger*; Ara tha, *Arabidopsis thaliana*; Bac sub, *Bacillus subtilis*; Bot cin, *Botrytis cinerea*; Cae ele, *Caenorhabditis elegans*; Chl rei, *Chlamydomonas reinhardtii*; Dan rer, *Danio rerio*; Dei rad, *Deinococcus radiodurans*; Dro mel, *Drosophila melanogaster*; Esc col, *Escherichia coli*; Gal gal, *Gallus gallus*; Gly max, *Glycine max*; Hom sap, *Homo sapiens*; Mar pol, *Marchantia polymorpha*; Met jan, *Methanocaldococcus jannaschii*; Med tru, *Medicago truncatula*; Neu cra, *Neurospora crassa*; Ory sat, *Oryza sativa*; Phy pat, *Physcomitrium patens*; Pha vul, *Phaseolus vulgaris*; Sac cer, *Saccharomyces cerevisiae*; Sel moe, *Selaginella moellendorffii*; Sol lyc, *Solanum lycopersicum*; Sol tub, *Solanum tuberosum*; Sus scr, *Sus scrofa*; Tri aes, *Triticum aestivum*; Ust may, *Ustilago maydis*; Vol car, *Volvox carteri*; Xen lae, *Xenopus laevis*; Zea may, *Zea mays*.

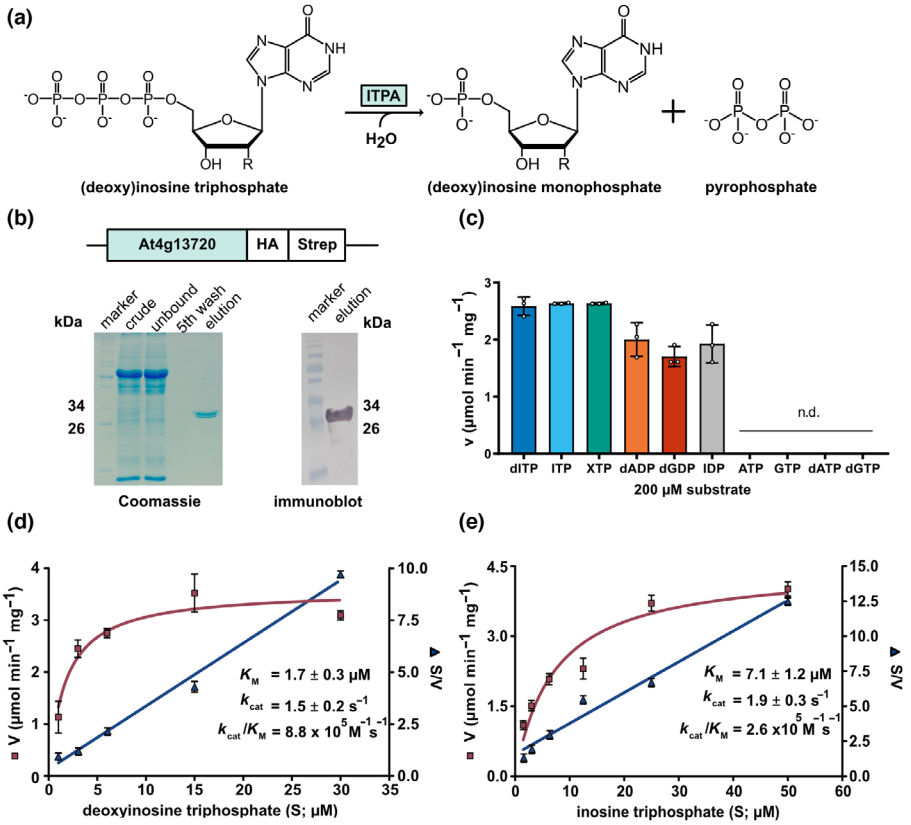

Fig. 2 Characterization of the enzymatic properties of inosine triphosphate pyrophosphatases (ITPA). (a) Reaction scheme of ITPA with inosine triphosphate (ITP). (b) Affinity purified, C-terminal Strep-tagged ITPA on a Coomassie-stained gel (left) and detection of Arabidopsis ITPA by immunoblotting using an antibody against the Strep-tag (right). Numbers indicate the respective size in kDa (kDa). Crude, centrifuged extract; unbound, centrifuged extract after incubation with Strep-Tactin matrix; 5th wash, supernatant after the fifth wash of the affinity matrix; elution, eluate of the affinity matrix. (c) Specific activity of ITPA with different substrate at a concentration of 200 µM. nd, not detected. (d) Determination of kinetic constants for the ITPA-catalyzed reaction of dITP to dIMP. Kinetic data were fitted using the Michaelis–Menten equation (orange) or by linear regression for the Hanes plot (S/V, purple). Error bars are standard deviation (SD), $n = 3$ reactions. S, substrate concentration; V, enzymatic activity. (e) The same as in (d), but using ITP as substrate. All *P*-values are provided in Table S4.

diphosphate (IDP), and XTP, as well as with deoxyadenosine diphosphate (dADP) and deoxyguanosine diphosphate (dGDP). In contrast to the ITPA from *H. sapiens*, the ITPA of *A. thaliana* efficiently dephosphorylates IDP (Davies *et al.*, 2012). For dITP and ITP, the kinetic constants were determined (Fig. 2d,e). With ITP as substrate, a K_M of 7.1 ± 1.2 µM and a turnover number of 1.9 ± 0.25 s^{-1} were measured. With dITP, the K_M was about fourfold lower at 1.7 ± 0.3 µM while the turnover number was similar at 1.5 ± 0.17 s^{-1}. Thus, Arabidopsis ITPA has catalytic efficiencies of 2.6×10^5 M^{-1} s^{-1} for ITP and 8.8×10^5 M^{-1} s^{-1} for dITP (Table 1).

ITPA mutants show an altered phenotype during senescence

To investigate the role of ITPA *in vivo*, two mutant lines and an overexpression line were created (Fig. S4). One T-DNA line with an insertion in an exon of *ITPA* was available from the SALK collection (SALK_053023; Fig. S4a).

We identified plants with a homozygous insertion of the T-DNA and observed that they lacked an intact transcript (Fig. S4b). This mutant was named *itpa-1*. A second line (*itpa-2*) was generated using CRISPR, resulting in a plant with two homozygous single base pair insertions causing frameshifts, one in exon 2 and one in exon 5. From the segregating population harboring the editing construct, *itpa-2* plants without the transgene were selected and used for further characterization. Both mutant lines had no obvious developmental phenotypes (Fig. S3a–d) but showed an early onset of senescence at 40 d after germination (Fig. 3a) and a slightly increased senescence at an age of 8 wk with *c.* 50% less chlorophyll in the oldest leaves, as well as an increased percentage of dead cells per leaf in *itpa* plants when compared to the WT (Fig. 3b–d). The plant fresh weight, the number of seeds per silique, and the length of the

Table 1 Comparison of kinetic parameters of plant, fungi, and mammal ITPA enzymes.

	ITPA (*Arabidopsis thaliana*; this study)			HAM1 (*Saccharomyces cerevisiae*; Davies *et al.*, 2012)			ITPA (*Homo sapiens*; Lin *et al.*, 2001)		
	K_M	k_{cat}	k_{cat}/K_M	K_M	k_{cat}	k_{cat}/K_M	K_M	k_{cat}	k_{cat}/K_M
Substrate	µM	s^{-1}	M^{-1} s^{-1}	µM	s^{-1}	M^{-1} s^{-1}	µM	s^{-1}	M^{-1} s^{-1}
dITP	1.7 ± 0.3	1.5 ± 0.17	8.8×10^5	3.06 ± 0.6	1.3	4.21×10^5	450 ± 100	360	1.16×10^6
ITP	7.1 ± 1.2	1.9 ± 0.25	2.6×10^5	2.38 ± 0.4	1.0	4.17×10^5	510 ± 100	580	1.14×10^6

±, standard deviation (SD). dITP, (deoxy)inosine triphosphate; ITP, inosine triphosphate; ITPA, inosine triphosphate pyrophosphatase.

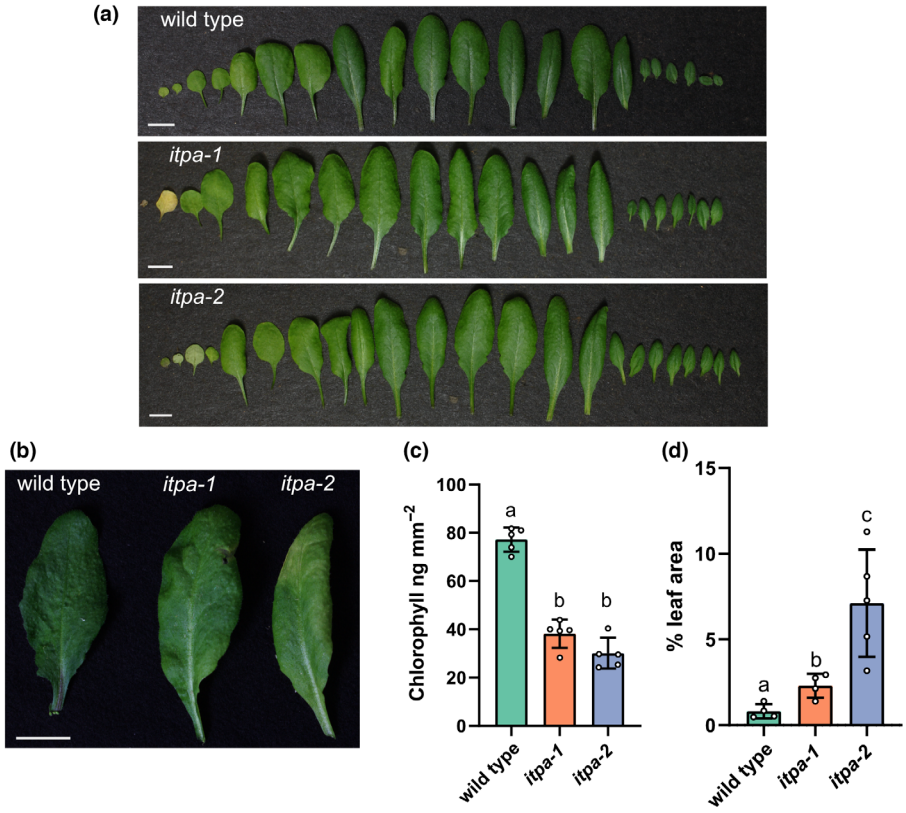

Fig. 3 Phenotypic comparison of wild-type (WT), *itpa-1*, and *itpa-2* plants. (a) Arabidopsis rosette leaves of 40-d-old WT, *itpa-1*, and *itpa-2* plants grown under long-day conditions. Bar, 10 mm. (b) Representative picture of the oldest leaves from 56-d-old plants of different genotypes used in (c). (c) Chlorophyll content of the respective oldest leaves from 56-d-old plants of different genotypes, $n = 5$. Every replicate represents a different plant of the same genotype. (d) Leaves of 56-d-old WT, *itpa-1*, and *itpa-2* plants were stained by Trypan blue, and dark pixels per leaf area were measured using ImageJ. Each open circle represents the result of measuring an independent biological replicate. Error bars are standard deviation (SD), $n = 4$–5. Statistical analysis was performed by a two-sided Tukey's pairwise comparison using the sandwich variance estimator. Different letters indicate $P < 0.05$. All *P*-values are provided in Table S4.

siliques were not different between the mutants and the WT (Fig. S3b–d).

ITPA is localized in the cytosol, nucleus, and putatively in plastids

To determine the subcellular localization of ITPA, cells of *N. benthamiana* co-expressing a C-terminally YFP-tagged variant of ITPA and cytosolic β-ureidopropionase C-terminally fused to CFP. Inosine triphosphate pyrophosphatase (ITPA) was clearly localized in the cytosol and nucleus, co-localizing with the cytosolic marker as the signals correlate with an *R*-value of 0.98; additionally, a good fit in the cross-correlation analysis was observed (Fig. 4a,b).

Both fusion proteins are stable as shown by an immunoblot (Fig. 4c). Interestingly, while the plastids are completely dark in the channel corresponding to the CFP signal of the cytosolic marker, there is signal in the YFP channel at these locations, illustrated by the arrows. Furthermore, the YFP signal and the plastidic autofluorescence overlap, indicated by a cyan coloration in the overlay of micrographs (Fig. 4a). Although the signals do not coincide completely, the data indicate that ITPA might also be localized in the plastids. This is in line with the predictions of several bioinformatic analysis tools summarized in the SUBA4 database, predicting nuclear, cytosolic, and plastidic localization for ITPA (Hooper *et al.*, 2017). Additionally, ITPA was found in a proteomic analysis of the plastid proteome (Kong *et al.*, 2011). A localization in mitochondria, also predicted by SUBA4, was not confirmed in our experiments.

ITPA is essential for the catabolism of ITP and IDP *in vivo*

In 35-d-old plants, IDP and ITP were only detectable in *itpa-1* and *itpa-2* background, but not in the WT (Fig. 5a).

Inosine triphosphate and IDP were reliably measured because they were baseline separated from the isobaric ATP and ADP isotopes (Fig. S5). The *itpa-1* and *itpa-2* lines contained 1.7 and 1.8 pmol g^{-1} IDP and 1.8 and 1.3 pmol g^{-1} ITP, respectively. This accounts for *c.* 30 molecules of ITP per 10^6 molecules of adenosine triphosphate (ATP) and between 300 and 400 molecules of IDP per 10^6 molecules of adenosine diphosphate (ADP, Table 2).

The ITP concentration per cell was *c.* 9.6 nM and that of IDP *c.* 11.2 nM estimated according to Straube *et al.* (2021). The IMP concentration was not altered significantly in the knockout lines (Fig. 5a), suggesting that ITP and IDP dephosphorylation is not a main contributor to the IMP pool. This is not surprising because IMP is a comparatively abundant intermediate of purine nucleotide biosynthesis and purine nucleotide catabolism, compared with the low abundant IDP and ITP (Baccolini & Witte, 2019; Witte & Herde, 2020). Although ITPA is active with dADP and dGDP *in vitro*, mutation of *ITPA* had no effect on the dADP and dGDP concentrations *in vivo* (Fig. S6a). The concentrations of other purine and pyrimidine nucleotides were also not altered in the mutant lines (Figs 5b, S6a–c).

What is the metabolic source of ITP and IDP?

Hitherto, the metabolic source of ITP and IDP is unknown. One possibility is that these metabolites arise from promiscuous

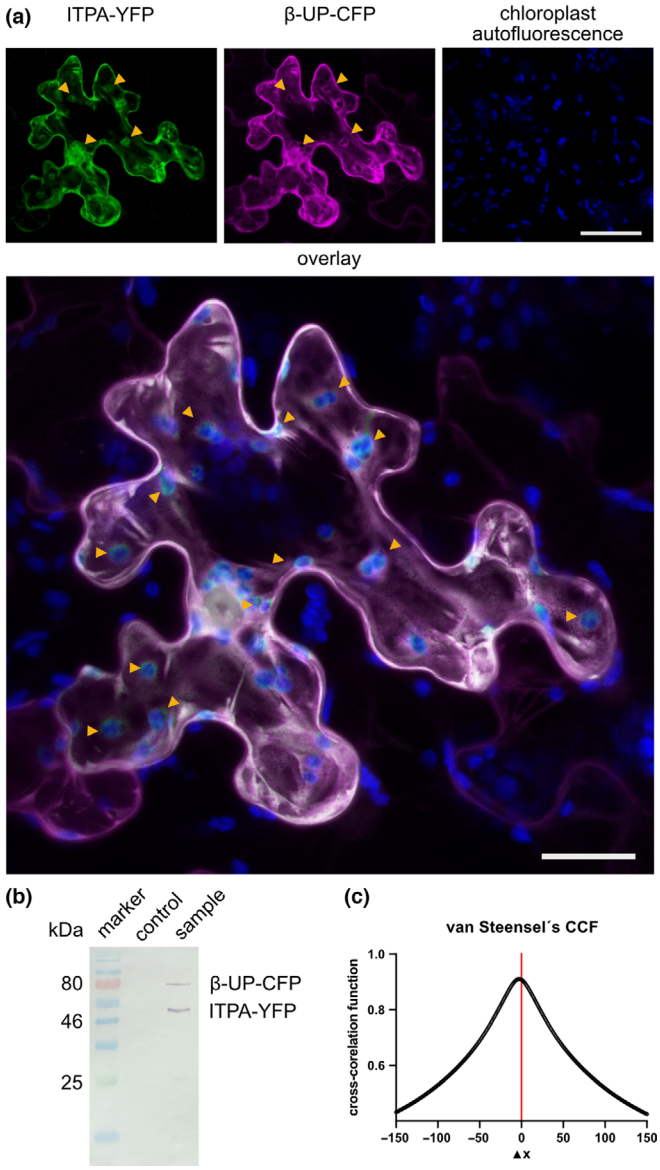

Fig. 4 Subcellular localization of inosine triphosphate pyrophosphatases (ITPA). (a) Confocal fluorescence microscopy images of leaf epidermal cells of *N. benthamiana* transiently co-expressing Arabidopsis ITPA C-terminally fused to YFP (ITPA-YFP) and cytosolic β-ureidopropionase C-terminally fused to CFP (β-UP-CFP). Left panel, YFP fluorescence; middle panel, CFP fluorescence; right panel, chloroplast autofluorescence. Bar, 50 μm. The large picture is an overlay of all three signals. Bar, 25 μm. Orange arrows indicate YFP signal not overlapping with the CFP signal. Analysis of the Pearson's correlation coefficient gave an *R*-value of 0.98 for the YFP and CFP signals. The images are representative for at least 10 micrographs of different cells. (b) Van Steensel's cross-correlation analysis for the YFP and CFP signals. (c) Analyzing the stability of the ITPA-YFP and β-UP-CFP by an immunoblot developed with a GFP-specific antibody. The control was generated from infiltrated leaves with *Rhizobium radiobacter* carrying the RNA silencing suppressor P19.

enzyme activity (Hanson *et al.*, 2016) of AMP kinases, which in addition to AMP may also be able to phosphorylate IMP. Consistent with this hypothesis, it has been shown in *E. coli* and *Saccharomyces cerevisiae* that an increase in the IMP content is concomitant with an accumulation of (deoxy)inosine in RNA and DNA (Pang *et al.*, 2012). In plants, more IMP could also lead to more ITP and IDP, which would indicate that the phosphorylation of IMP by kinases is a source of ITP and IDP.

A biochemical approach was used to investigate the question of possible aberrant IMP phosphorylation. We determined the enzymatic activities of the two cytosolic AMP kinases, AMPK3 (At5g50370) and AMPK4 (At5G63400) of *A. thaliana* with either 1 mM AMP or IMP as substrates (Lange *et al.*, 2008; Chen *et al.*, 2018; Fig. 6a,b). Although IMP is an *in vitro* substrate for both enzymes, the activity with IMP was only 3.9% of that with AMP for AMPK3 (Fig. 6a) and 5.2% for IMP vs AMP for AMPK4 (Fig. 6b).

In vivo the relative activity with IMP will be lower because the cellular IMP pool is several orders of magnitude smaller than that of AMP. Nonetheless, the data show that AMPKs can phosphorylate IMP in principle resulting in the formation of ITP and IDP.

To further test the hypothesis of spurious IMP phosphorylation as a source for IDP and ITP, we fed ribavirin to *A. thaliana* WT, *itpa-2*, and *itpa-2::C* plants (Fig. 7), an inhibitor of IMP DEHYDROGENASE (IMPDH, Keya *et al.*, 2003). This enzyme represents a major sink of IMP in plant metabolism (Witte & Herde, 2020), and its inhibition likely increases the IMP concentration *in vivo* and thus the availability of substrate for spurious phosphorylation by AMPKs (Fig. 7c). Ribavirin treatment for 24 h caused a significant increase in the IMP content in ribavirin-treated *A. thaliana* seedlings compared with the mock-treated samples and a decreased concentration of downstream metabolites like XMP (Fig. 7). We noticed a higher abundance of IMP in ribavirin-treated *itpa-2::C* plants and suspect that this is a result of a higher abundance of ITPA, as ITPA from other organisms is described dephosphorylate ribavirin triphosphate (RTP) to its respective monophosphate (Vidal *et al.*, 2022). In the overexpression line, this leads to an increased concentration of ribavirin monophosphate, which is the inhibitory metabolite of IMPDH. Instead of RTP being incorporated into RNA, it is dephosphorylated, leading to an even stronger block of IMPDH and thus a greater accumulation of IMP.

Concomitant with higher IMP concentrations, the abundance of IDP and ITP was increased in all genotypes treated with ribavirin (Fig. 7b), suggesting that spurious phosphorylation of IMP cannot be excluded as a source of IDP and ITP despite the comparably low activity of AMP kinases with IMP as a substrate. The concentration of IDP and ITP was significantly decreased in *itpa-2::C* plants compared with the WT and *itpa-2* plants demonstrating a gain-of-function concerning IDP/ITP dephosphorylation caused by ectopic expression of *ITPA*.

We used the ribavirin treatment as a tool to extend the concept of IMP phosphorylation to other plant species and developmental stages. Thus, we infiltrated *N. benthamiana* plants with ribavirin and the mock control (Fig. S7), similarly to Arabidopsis, the treatment with ribavirin led to increased concentrations of IMP, whereas XMP was not detected (Fig. S7). However, in *N. benthamiana*, the treatment did not result in increased IDP and ITP concentrations, suggesting that the contribution of spurious IMP phosphorylation to IDP and ITP pools varies between

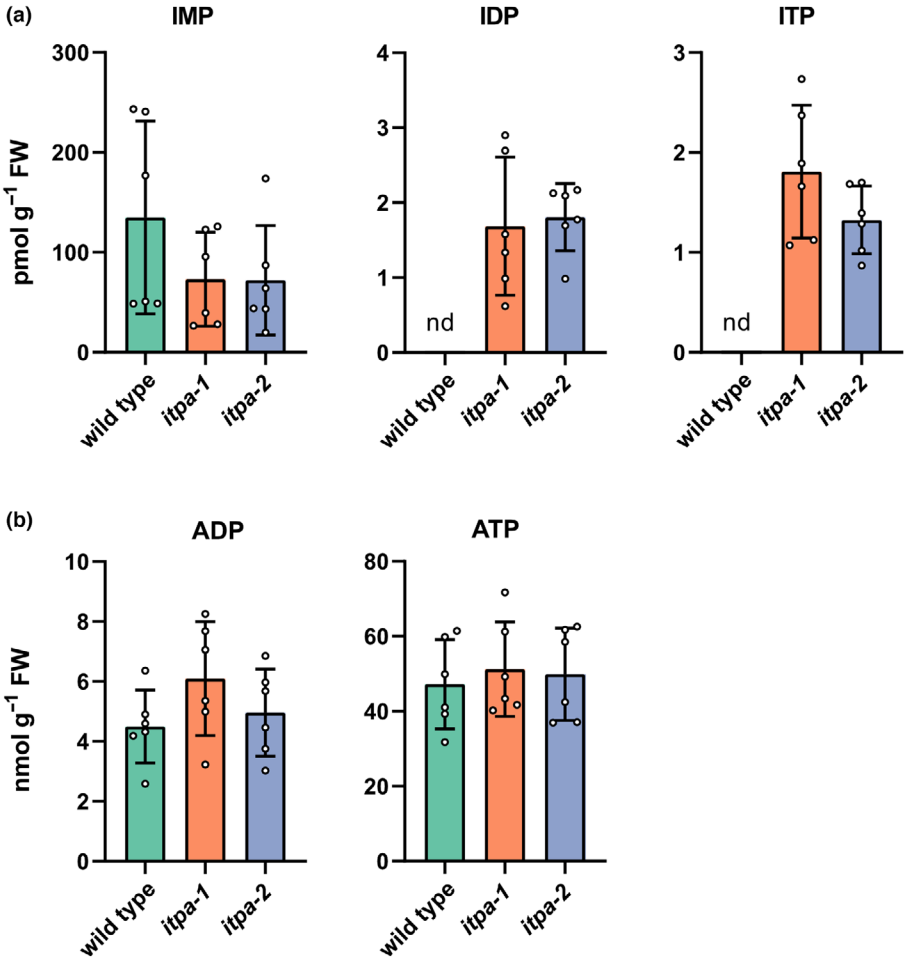

Fig. 5 Loss-of-function of *itpa* causes an accumulation of inosine diphosphate (IDP) and inosine triphosphate (ITP), while adenylate concentrations remain unchanged. (a) Concentrations of inosylates in rosette leaves of 35-d-old Arabidopsis wild-type (WT), *itpa-1*, and *itpa-2* plants. (b) As in (a) but for adenosine diphosphate (ADP) and adenosine triphosphate (ATP). Each open circle represents the result of measuring an independent biological replicate. Error bars are standard deviation (SD), $n = 6$. Every replicate represents a different plant. Statistical analysis was performed by a two-sided Tukey's pairwise comparison using the sandwich variance estimator. Different letters indicate $P < 0.05$. All *P*-values are provided in Table S4. nd, not detected.

Table 2 Ratios of ITP and IDP per million molecules of ATP and ADP, respectively.

	itpa-1	*itpa-2*
ITP/1 × 10^6 ATP	36.6 ± 12	28.7 ± 11
IDP/1 × 10^6 ADP	300.8 ± 162	407.5 ± 178

±, standard deviation (SD). ADP, adenosine diphosphate; ATP, adenosine triphosphate; IDP, inosine diphosphate; ITP, inosine triphosphate.

plant species (Arabidopsis and Nicotiana) or developmental stages (seedlings and fully developed leaves).

Aberrant metabolites can also be derived from nonenzymatic processes – e.g. from contact with ROS (Hanson *et al.*, 2016; Lerma-Ortiz *et al.*, 2016). Heavy metals, such as cadmium, are known to cause ROS production in plants and comprise important anthropogenic pollutants (Di Sanità & Gabbrielli, 1999; Cho & Seo, 2005; Lin *et al.*, 2007). It has been well established that cadmium-induced oxidative stress not only damages macromolecules such as the DNA directly but also causes an increased rate of lipid peroxidation (Lin *et al.*, 2007). To test whether this oxidative stress also has an impact on nucleotides, we grew WT and *itpa-1* plants hydroponically for 14 d and applied cadmium sulfate (0 and 10 µM). Without Cd, WT plants only accumulated small amounts of ITP, but with 10 µM Cd the ITP content rose significantly (Fig. 8). Inosine diphosphate was not detectable in the WT. As expected, the mutant generally contained more IDP and ITP than the WT and the application of Cd resulted in a further increase in these pools. The concentrations of ITP and IDP measured in this experiment in 14-d-old plants grown in a hydroponic system were comparable to those in 35-d-old plants grown on soil (Figs 5a, 8). These data show that ITP and IDP can be formed under stress conditions that involve ROS probably by the deamination of ATP and ADP. Overall, our data suggest that spurious IMP phosphorylation and ATP deamination caused by oxidative stress both can contribute to IDP and ITP pools but the impact of both processes depends on environmental conditions and putatively on the developmental context.

ITPA prevents (d)ITP incorporation into DNA and RNA

Measuring deoxyinosine (dI) in digested DNA of 7-d-old plants by liquid chromatography-mass spectrometry (LC–MS) revealed that both mutant lines accumulate dI in the DNA (Fig. 9a). Wild-type (WT) DNA contained 290 ± 96 dI per million molecules deoxyadenosine (dA). This amount was more than doubled in the mutants (Table S6). In DNA from older plants (56 d), dI

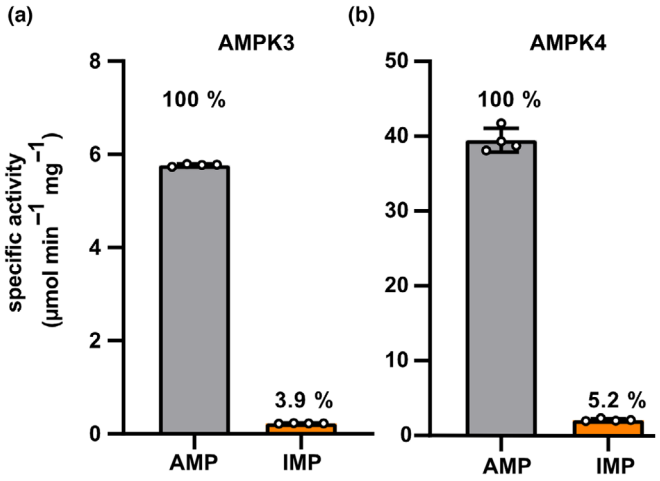

Fig. 6 Enzymatic activity of AMPK 3 and 4 with adenosine monophosphate (AMP) and inosine monophosphate (IMP). Arabidopsis enzymes were transiently expressed in *Nicotiana benthamiana* as C-terminal Strep-tagged variants and affinity purified. (a) Specific activity of AMPK3 with 1 mM AMP or IMP in the presence of 1 mM ATP. Linear rates were observed in all cases. Error bars are standard deviation (SD). Each open circle represents the result of measuring a replicate, each replicate represents an independent enzyme assay from the same enzyme preparation ($n = 4$). (b) Analogous data for AMPK4.

could not be detected in the WT and accumulated in DNA of the mutants to approximately the same level as in seedlings. Therefore, a marked increase in dI accumulation in DNA with age could not be observed. Interestingly, the higher dI concentration in DNA of *itpa* plants demonstrates that a dITP pool likely exists in plants. Deoxyxanthosine was not detected in DNA. To test whether the concentration of dI is really dependent on *ITPA* expression, we analyzed the concentration of dI in DNA of 7-d-old WT, *itpa-2*, and *itpa-2::C* plants grown hydroponically (Fig. 9b).

Consistently, itpa-2 plants accumulated dI and the overexpression of ITPA (itpa-2::C) led to a concentration of dI comparable to what was measured in WT plants.

In digested total RNA of 35-d-old plants, 405 ± 117 molecules of inosine per million molecules of adenosine were detected (Fig. 9c). The *itpa* lines contained about twofold more inosine in the RNA (Table S6), showing that also the RNA is protected by ITPA. In a pilot experiment, the RNA of younger, 21-d-old plants was analyzed and contained only 200 molecules of inosine per million molecules of adenosine (Fig. S8), which is about half the amount found in 35-d-old plants. A similar tendency was observed for the *itpa-1* line. In contrast to deoxyinosine in DNA, it appears that the inosine content of RNA increases with age. Interestingly, inosine-containing RNA can be specifically recognized and cleaved by an endonuclease in Arabidopsis, which may limit the amount of inosine that can accumulate in RNA (Endo *et al.*, 2021). Xanthosine was not detected in RNA. In summary, the data demonstrate that ITPA is an enzyme required for the removal of dITP and ITP to protect DNA and RNA from random incorporation of (deoxy)inosine (Fig. 10).

Loss of ITPA leads to an upregulation of transcripts involved in biotic stress

We further investigated whether the loss of *ITPA* leading to the accumulation of (deoxy)inosine in nucleic acids and inosylates in nucleotide pools has an influence on the transcriptome. An RNA-seq analysis was performed with RNA isolated from rosette leaves of 35-d-old WT and *itpa-1* plants that had been grown side-by-side in a randomized fashion and for which we had already confirmed differential levels of inosine in RNA (Fig. 9c). Plants lacking ITPA showed an upregulation of 256 transcripts and a downregulation of only 28 transcripts at a $\log_2$ fold change ($\log_2$ FC) of ≥ 2 and ≤ -2, respectively, in addition to a false discovery rate (FDR) of ≤ 0.05 (Table S2). Many regulated transcripts were involved in biological processes associated with stress responses and often encode proteins with kinase activity or transcription factors as reported by GO (gene ontology) enrichment analysis (Fig. S9; Table S3). Upon closer inspection, we found that especially transcripts related to the SA response (Fig. 11a), SAR (Fig. 11b), and aging (Fig. 11c) were upregulated.

Since the transcriptional profiles suggested that the concentration of SA is altered, we quantified it. Significantly higher SA concentrations were found in 35-d-old plants lacking ITPA compared with the corresponding WT (Fig. 11d).

Consistent with public data sets (Winter *et al.*, 2007), the expression of *ITPA* itself was not influenced by a treatment with SA (Fig. 11e), but treating WT plants with cadmium sulfate resulted in a minor, but significant, decrease in ITPA transcript abundance (Fig. 11e). Although counter-intuitive, a reduced expression of ITPA in oxidatively stressed plants has been reported recently (Arruebarrena Di Palma *et al.*, 2022). During development, the abundance of the ITPA transcript is decreasing (Fig. 11f), which is also in accordance with publicly available data (Winter *et al.*, 2007).

Discussion

Although the existence of ITPA in plants has been suggested based on sequence comparisons (Lin *et al.*, 2001; James *et al.*, 2021), these *in silico* predictions have never been experimentally tested nor has an *itpa* mutant been characterized in any plant species. Here, we demonstrate that plants have ITPA and that it is involved in the metabolite damage repair system in Arabidopsis. The kinetic properties of the enzyme from Arabidopsis are similar to those of the yeast ortholog HAM1p. Interestingly, the human ITPA has a 250-fold higher K_M and a 300- to 500-fold greater catalytic activity than the plant and yeast enzymes (Table 1), which might be an adaptation to high ITP concentrations in some human cells, for example, erythrocytes (Behmanesh *et al.*, 2009). However, in other human cells, the ITP concentration must be relatively low because it was generally not detectable (Sakumi *et al.*, 2010).

The K_M of Arabidopsis ITPA for ITP of 7.1 µM is *c.* 1000-fold higher than the cellular concentration of ITP (9.6 nM) determined in *itpa* background, which will be even lower in the WT. We were unable to detect dITP but could show that

New Phytologist

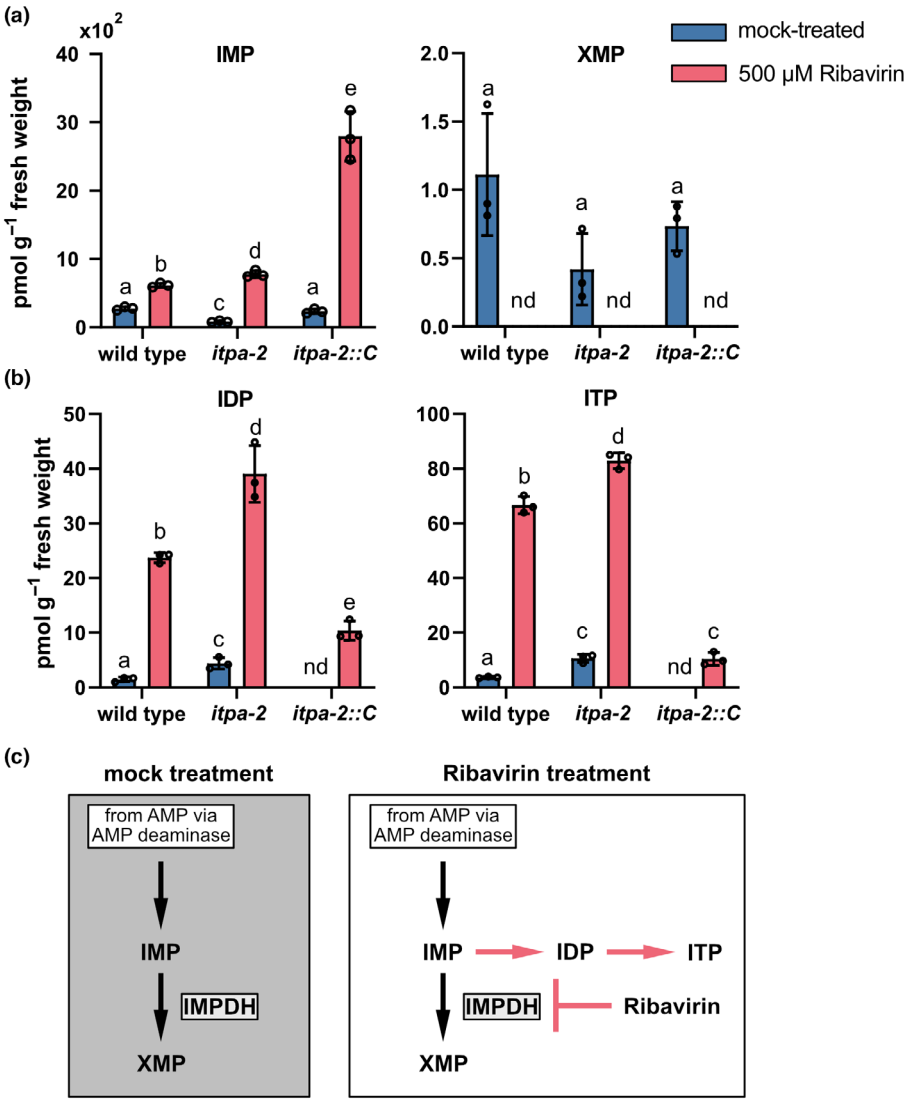

Fig. 7 Manipulation of inosine monophosphate (IMP) content in 7-d-old *Arabidopsis thaliana* plants alters the concentration of xanthosine monophosphate (XMP), inosine diphosphate (IDP), and inosine triphosphate (ITP). (a) Concentrations of IMP and XMP in 7-d-old Arabidopsis wild-type (WT), *itpa-2*, and *itpa-2::C* plants, grown hydroponically. Plants were either mock-treated or treated with 500 µM ribavirin for 24 h. (b) as in (a) but for IDP and ITP. Each open circle represents the result of measuring an independent biological replicate. Error bars are standard deviation (SD), $n = 3$. Every replicate represents a pool of seedlings from a different hydroponic vessel. Statistical analysis was performed by a two-sided Tukey's pairwise comparison using the sandwich variance estimator. Different letters indicate $P < 0.05$. All *P*-values are provided in Table S4. nd, not detected. (c) model of metabolic flux of parts of the purine metabolism in mock-treated and ribavirin-treated plants. Black arrows indicate the flux of purine metabolites in mock-treated plants, whereas red arrows indicate the proposed flux of purine metabolites in ribavirin-treated plants. The blunt-ended red arrow displays the inhibition of IMP DEHYDROGENASE (IMPDH) by ribavirin.

mutation of *ITPA* led to more deoxyinosine in DNA. Thus, dITP is likely an *in vivo* substrate of ITPA (K_M = 1.7 µM for dITP). We estimate that the dITP concentration is in the low pM range, assuming that the ratio of ITP to dITP is comparable to the ATP-to-dATP ratio of *c.* 500 to 1000 (Straube *et al.*, 2021). A difference in several orders of magnitude between K_M and cellular substrate concentration is also known for other housekeeping enzymes (Galperin *et al.*, 2006; Yoshimura *et al.*, 2007; Sakumi *et al.*, 2010; Heinemann *et al.*, 2021). Furthermore, it has been shown that a K_M above cellular concentrations of a metabolite seems to be typical for enzymes in *E. coli* involved in the degradation of nucleotides (Bennett *et al.*, 2009).

Xanthosine triphosphate, dXTP, and (deoxy)xanthosine in nucleic acids could not be detected, indicating that the deamination of (deoxy)guanosine in DNA and RNA and the phosphorylation of (d)XMP are very rare. Therefore, ITPA seems mainly involved with ITP and IDP and somewhat with dITP dephosphorylation *in vivo* (Fig. 10). The activity of Arabidopsis ITPA with IDP is interesting, since the yeast and human orthologs have a rather poor activity with IDP (Holmes *et al.*, 1979; Davies *et al.*, 2012). Human cells possess a nudix hydrolase (NUDT16), which hydrolyzes preferably IDP and dIDP, acting synergistically with ITPA to protect cells from high levels of (d)ITP (Abolhassani *et al.*, 2010). This enzyme is missing in Arabidopsis, which may explain why the plant enzyme is also an efficient diphosphate hydrolase. IDP is likely the product of ADP deamination (Fig. 8), and ADP is also a substrate of the ribonucleotide reductase (RNR; Wang & Liu, 2006), an enzyme complex catalyzing the first committed step in the synthesis of deoxyribonucleotide triphosphates. Assuming that RNR accepts IDP as a substrate, the reaction would lead to the formation of deoxyinosine diphosphate, which could be phosphorylated and then be incorporated into DNA.

According to our data, an important source of ITP is probably the deamination of ATP. The concentration of the adenylates is by far the highest of all nucleotides (Straube *et al.*, 2021), and even a small rate of deamination will generate significant amounts of ITP. Additionally, this rate can be enhanced by

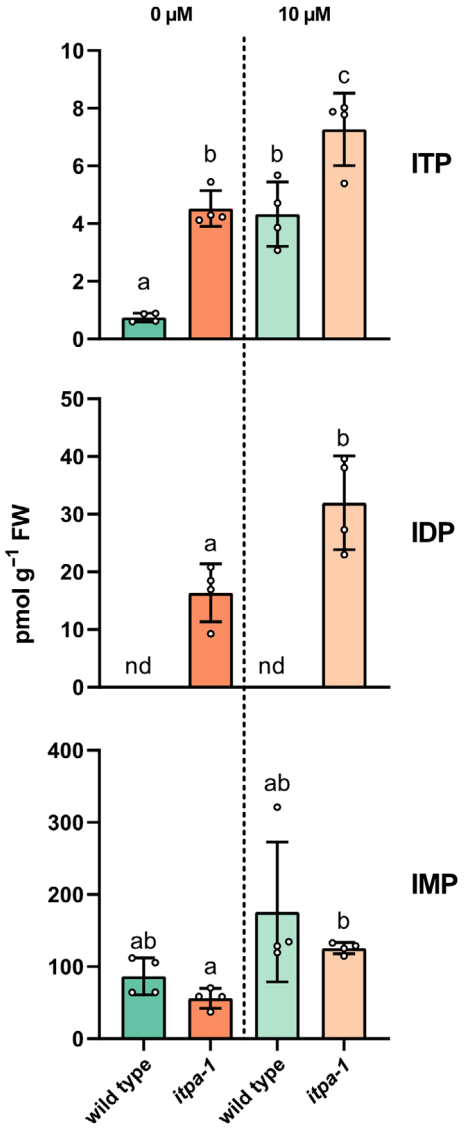

Fig. 8 Effect of cadmium causing oxidative stress on inosylate concentrations. Arabidopsis mutant and wild-type (WT) plants grown in a hydroponic system for 14 d were treated with 10 µM cadmium sulfate for 24 h or were left untreated. inosine triphosphate (ITP), inosine diphosphate (IDP), and inosine monophosphate (IMP) were quantified. Each open circle represents the result of measuring an independent biological replicate. Error bars are standard deviation (SD), $n = 4$. Every replicate represents a pool of plants from an independent hydroponic vessel. Statistical analysis was performed by a two-sided Tukey's pairwise comparison using the sandwich variance estimator. Different letters indicate $P < 0.05$. All P-values are provided in Table S4. nd, not detected.

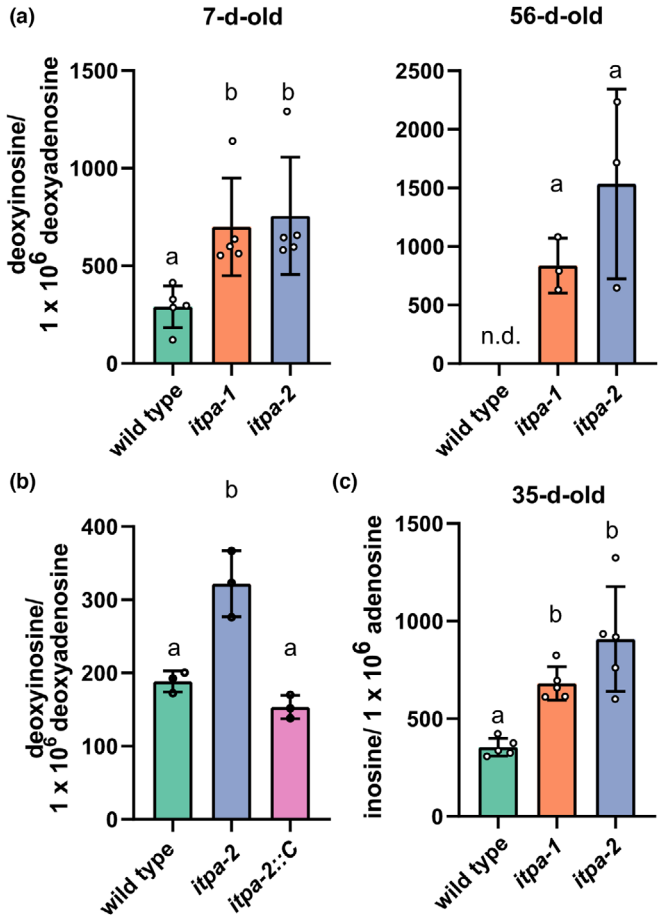

Fig. 9 Concentration of deoxyinosine and inosine in nucleic acids of different genotypes. (a) Molecules of deoxyinosine per million molecules of deoxyadenosine in DNA isolated from pools of 7-d-old Arabidopsis seedlings grown on agar plates and 56-d-old Arabidopsis rosettes. Error bars are standard deviation (SD), $n = 5$ and 3. (b) Molecules of deoxyinosine per million molecules of deoxyadenosine in DNA isolated from pools of 7-d-old Arabidopsis seedlings grown hydroponically. Each open circle represents the result of measuring an independent biological replicate. Error bars are SD, $n = 3$. (c) Molecules of inosine per million molecules adenosine in total RNA isolated from 35-d-old Arabidopsis rosettes. Error bars are SD, $n = 5$. Every replicate represents a different plant. Statistical analysis was performed by a two-sided Tukey's pairwise comparison using the sandwich variance estimator. Different letters indicate $P < 0.05$. All P-values are provided in Table S4. nd, not detected.

oxidative stress, which can occur in plant cells because of abiotic and biotic stress. AMP kinases may also contribute to the IDP and ITP pool because they can use IMP as substrate albeit with lower activity than for AMP. The possibility of spurious phosphorylation by kinases involved in nucleotide metabolism has been discussed recently (Chen *et al.*, 2018; Chen & Witte, 2020). However, *in vivo* there is far more AMP than IMP and our manipulation of IMP in *N. benthamiana* leaves showed no correlation between IMP and ITP concentrations (Fig. S7). However, in 7-d-old *A. thaliana* plants, the concentrations of IDP and ITP rose significantly when plants were treated with ribavirin. We hypothesize that this discrepancy is due to a different developmental context, as there is likely more overall nucleotide kinase activity in developing tissues than in fully developed leaves (Niehaus *et al.*, 2022), which would also increase the rate of spurious IMP phosphorylation.

It is surprising that ITPA is only located in the cytosol, nucleus, and plastids but not in the mitochondria because ATP occurs in each of these compartments and mitochondria also perform nucleic acid biosynthesis. Additionally, the respiratory chain and photosystems are the main sources for ROS in plant cells (Janků *et al.*, 2019), potentially leading to nucleotide and nucleic acid damage, such as nucleotide deamination (Cadet &

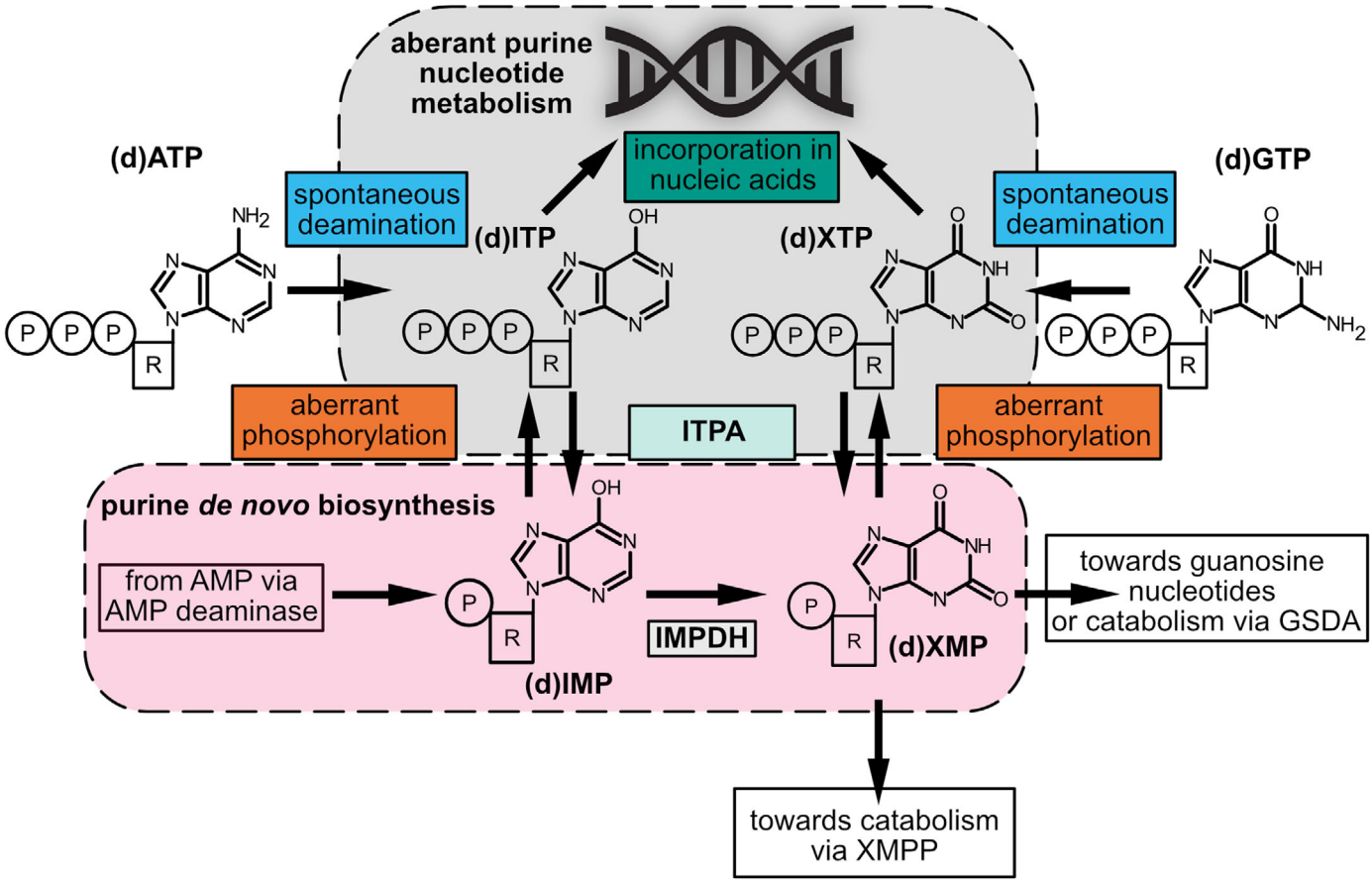

Fig. 10 Overview of deaminated purine nucleotide metabolism and its interplay with purine *de novo* synthesis. Enzymatic and nonenzymatic steps that lead to the generation of deaminated purine nucleotides are shown, as well as their removal by the inosine triphosphate pyrophosphatase (ITPA) and reintegration into canonical purine nucleotide metabolism or potential incorporation into nucleic acids. AMP, adenosine monophosphate; (d)ATP, (deoxy) adenosine triphosphate; (d)ITP, (deoxy)inosine triphosphate; (d)XTP, (deoxy)xanthosine triphosphate; (d)GTP, (deoxy)guanosine triphosphate; (d)IMP, (deoxy)inosine monophosphate; (d)XMP, (deoxy)xanthosine monophosphate; IMPDH, inosine monophosphate dehydrogenase; XMPP, xanthosine monophosphate phosphatase.

Wagner, 2013), in mitochondria and plastids, respectively (Tripathi *et al.*, 2020). It is known that ATP and ADP are rapidly exchanged over the mitochondrial membrane because the mitochondria supply the cell with ATP produced by oxidative phosphorylation (Braun, 2020). Therefore, cytosolic ITPA may be able to also purify the mitochondrial adenylate pool – this however implies that ITP and IDP are also rapidly exchanged over the mitochondrial membrane (Haferkamp *et al.*, 2011). By contrast, plastids exchange adenylates with the cytosol mainly at night for ATP import whereas during the day they internally generate ATP from ADP driven by photosynthesis for triosephosphate production. Plastids may require their own ITPA because in the light ROS production is high and adenylates are not exchanged with the cytosol.

Mutant plants lacking *ITPA* show a slightly earlier senescence and increased cell death (Fig. 3a–d). This is a relatively moderate phenotype compared to what occurs in mammals. Mice without functional ITPA die shortly after birth (Behmanesh *et al.*, 2009). A null mutation of *ITPA* in humans leads to severe developmental abnormalities and is also lethal (Handley *et al.*, 2019). Humans with missense mutations in *ITPA* develop severe side effects when treated with purine analog like ribavirin or thiopurines (Simone *et al.*, 2013). By contrast, the single-cell eukaryote *S. cerevisiae* and also the model bacterium *E. coli* show no particular physiological phenotype when they lack ITPA (Pavlov, 1986; Clyman & Cunningham, 1987; Noskov *et al.*, 1996). Nonetheless, the *E. coli* mutant has an induced SOS response, a pathway that is turned on by DNA damage (Clyman & Cunningham, 1987).

In contrast to other housekeeping genes, a decrease in *ITPA* transcript abundance is observed during senescence (Fig. 11f). The housekeeping function of ITPA is centered on the proofreading of damaged metabolites, which is likely not as important in senescent plants as it is in developing tissues. Consistently, other metabolite damage repair enzymes, like NUDX1 (AT1G68760), show a similar expression profile during development (Winter *et al.*, 2007).

So why do plants lacking ITPA activity show symptoms of early senescence? This could be related to the accumulation of (deoxy)inosine in DNA and RNA in the mutant (Figs 9, S8). Deaminated purines in RNA were shown to lead to reduced polymerase fidelity, RNA structure changes, altered stability and

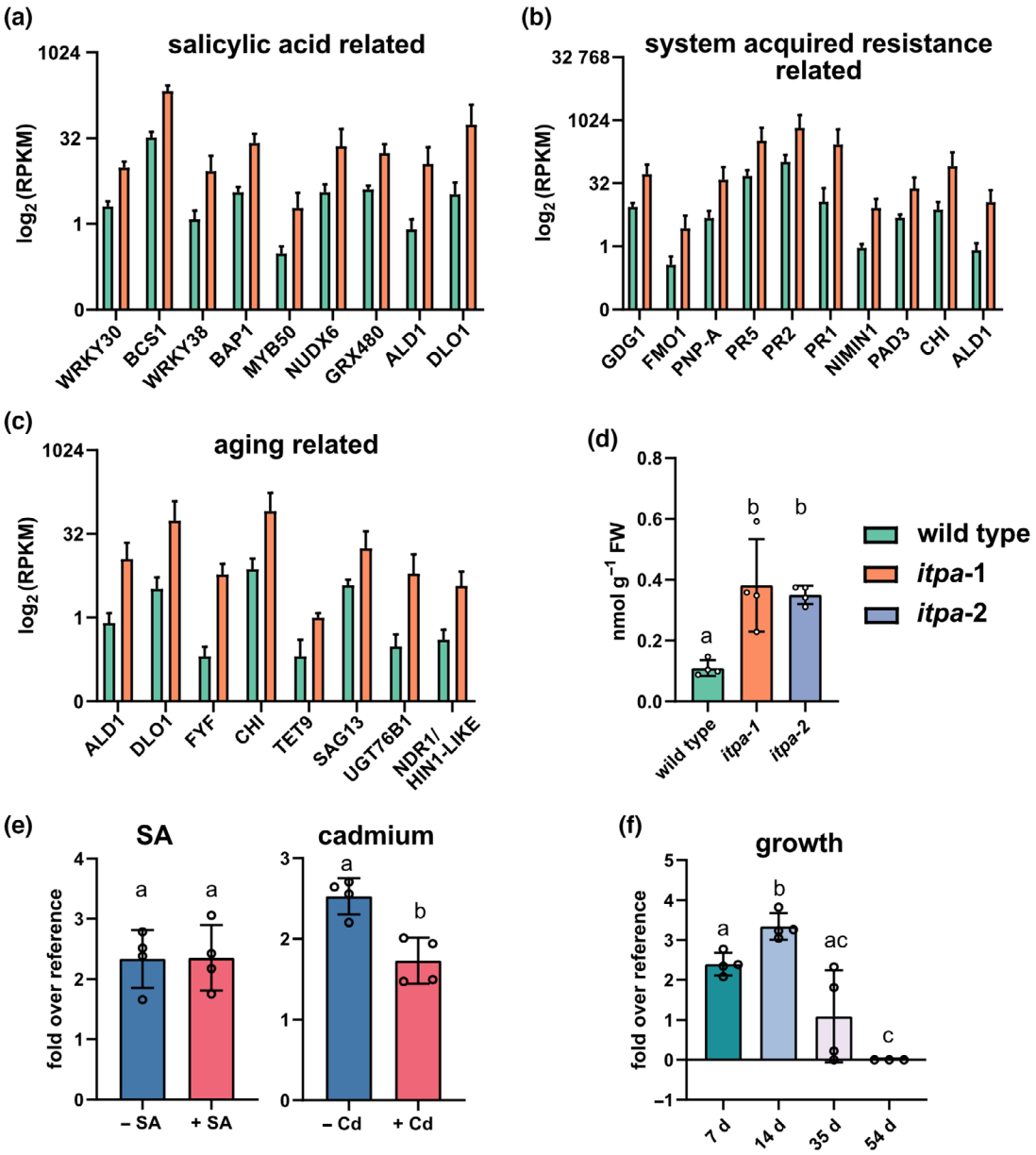

Fig. 11 Loss-of-function of inosine triphosphate pyrophosphatase (ITPA) leads to differential upregulation of transcripts associated with salicylic acid (SA), systemic acquired resistance (SAR) as well as aging and increased endogenous concentrations of SA. (a) RNA was isolated from 35-d-old Arabidopsis rosettes and analyzed by RNA-seq. Log_2 (RPKM) values are shown for genes associated with response to SA (GO:0009751) and differentially regulated between wild-type (WT) and *itpa-1* samples. Error bars are standard deviation (SD), $n = 3$. Every replicate represents a pool of two different plants. (b) As in (a) but for genes associated with SAR (GO:0009627). (c) As in (a) but for genes associated with aging (GO:0007568). (d) Concentrations of SA in 35-d-old Arabidopsis rosettes analyzed by LC–MS. Error bars are SD, $n = 4$. Every replicate represents a different plant. (e) Transcript abundance of the ITPA transcript in 14-d-old *A. thaliana* WT plants grown hydroponically. Plants were either mock-treated, treated with 1 mM SA or 500 μM cadmium sulfate for 24 h. Every replicate represents a pool of seedlings from a different hydroponic vessel. (f) ITPA transcript abundance in *A. thaliana* WT plants grown on soil for 7, 14, 35, or 54 d. Each open circle represents the result of measuring an independent biological replicate. Error bars are SD, $n = 3$–4. Every replicate represents a different plant, only in case of 7-d-old plants seedlings were pooled for RNA isolation. Statistical analysis was performed by a two-sided Tukey's pairwise comparison using the sandwich variance estimator. Different letters indicate $P < 0.05$. All *P*-values are provided in Table S4.

mistranslation (Thomas *et al.*, 1998; Ji *et al.*, 2017; Schroader *et al.*, 2022), and in case of DNA to mutations (Spee *et al.*, 1993; DeVito *et al.*, 2017) and genome instability (Yoshimura *et al.*, 2007). We observed a higher amount of inosine in RNA of older *itpa* plants (Figs 9, S8), indicating that the problems may become more severe with age. DNA damage can lead to programmed cell death (PCD) in Arabidopsis (Wang & Liu, 2006), and we saw a higher incidence of PCD in the *itpa* background during senescence (Fig. 3d). An early senescence phenotype similar to that in *itpa* plants was also observed in plants with a higher frequency of unrepaired DNA double-strand breaks (Li *et al.*, 2020). In summary, damage to DNA and RNA by aberrant nucleotide incorporation may be the cause for the earlier senescence and the increased PCD rate. Alternatively, the detrimental

effects of *ITPA* mutation may also be unrelated to the alteration of nucleic acids but caused by ITP accumulation. ITP can directly influence cellular processes that either require or are inhibited by ATP or GTP (Vanderheiden, 1979; Osheroff *et al.*, 1983; Klinker & Seifert, 1997; Burton *et al.*, 2005). However, compared with the sizes of the ATP and GTP pools, the ITP pool is very small even in the *itpa* background, which argues against a direct metabolic interference of ITP.

The abundance of transcripts associated with SA, senescence, and SAR increases in *itpa* plants, and they accumulate SA (Figs 11, S9). Mutants with constitutive high levels of SA are known to senesce prematurely. The higher SA levels in *itpa* plants may thus present an explanation for the early senescence phenotype observed (Fig. 3a–d) and may affect plant–pathogen interactions. How the mutation of ITPA and the induction of SA are connected is unclear. We hypothesize that an accumulation of deoxyinosine in DNA causes more DNA repair and turnover associated with occasional double-strand breaks. It is known that in plants with more unrepaired DNA double-strand breaks the concentration of SA is increased (Li *et al.*, 2020). It also has been shown that SA can trigger DNA damage (Hadwiger & Tanaka, 2017) and that proteins involved in DNA damage response, like RAD51, interact synergistically to trigger increased transcription of genes involved in plant immunity (Yan *et al.*, 2013). Taken together, it is possible that the transcripts involved in SA response, SAR, and aging are upregulated as a consequence of DNA damage.

Deamination of adenylates is an unavoidable chemical reaction, and most organisms including plants have ITPA to protect their nucleic acids from the reaction products. Whether (d)ITP and (d)IDP are more than just an undesirable metabolic byproduct remains to be investigated.

Acknowledgements

We would like to express our gratitude to Holger Eubel and Björn Heinemann for providing the hydroponic system and André Specht for technical assistance. We also like to thank Anke Steppuhn (University of Hohenheim) for the donation of the phytohormone isotope standards. We furthermore like to express our gratitude to Sören Budig and Frank Schaarschmidt (Leibniz University, Hannover) for advice on the statistical analysis. We like to acknowledge the support by the Deutsche Forschungsgemeinschaft (grant no. HE 5949/4-1 to MH), (grant no. WI3411/7-1 and WI3411/8-1 to C-PW), and (grant no. INST 187/741-1 FUGG). Open Access funding enabled and organized by Projekt DEAL.

Competing interests

None declared.

Author contributions

HS and MH designed the research; HS, JS, LF, JR and MN performed the research; HS, JS, LF, JR, MN and MH analyzed the data, and HS, CPW and MH interpreted the data; HS, CPW and MH wrote the manuscript. All authors read and revised the manuscript and agreed on the final version.

ORCID

Lisa Fischer https://orcid.org/0000-0001-5033-2490
Marco Herde https://orcid.org/0000-0003-2804-0613
Markus Niehaus https://orcid.org/0000-0003-3057-7823
Jannis Rinne https://orcid.org/0000-0003-0361-5257
Henryk Straube https://orcid.org/0000-0001-9286-7784
Jannis Straube https://orcid.org/0000-0002-6813-3809
Claus-Peter Witte https://orcid.org/0000-0002-3617-7807

Data availability

The data that support the findings of this study are available in the Supporting Information of this article. Information about the mutant lines in this article can be obtained in the GenBank/EMBL data libraries under the following accession number: At4g13720 (ITPA). Raw read data from Illumina sequencing are deposited at the Sequence Read Archive (SRA) on NCBI under the following accession number: PRJNA807491.

References

Abolhassani N, Iyama T, Tsuchimoto D, Sakumi K, Ohno M, Behmanesh M, Nakabeppu Y. 2010. NUDT16 and ITPA play a dual protective role in maintaining chromosome stability and cell growth by eliminating dIDP/IDP and dITP/ITP from nucleotide pools in mammals. *Nucleic Acids Research* **38**: 2891–2903.

Alonso JM, Stepanova AN, Leisse TJ, Kim CJ, Chen H, Shinn P, Stevenson DK, Zimmerman J, Barajas P, Cheuk R *et al.* 2003. Genome-wide insertional mutagenesis of *Arabidopsis thaliana*. *Science* **301**: 653–657.

Arruebarrena Di Palma A, Perk EA, Carboni ME, Garcia-Mata C, Budak H, Tör M, Laxalt AM. 2022. The isothiocyanate sulforaphane induces respiratory burst oxidase homologue D-dependent reactive oxygen species production and regulates expression of stress response genes. *Plant Direct* **6**: e437.

Baccolini C, Witte C-P. 2019. AMP and GMP catabolism in Arabidopsis converge on xanthosine, which is degraded by a nucleoside hydrolase heterocomplex. *Plant Cell* **31**: 734–751.

Batista-Silva W, Heinemann B, Rugen N, Nunes-Nesi A, Araújo WL, Braun H-P, Hildebrandt TM. 2019. The role of amino acid metabolism during abiotic stress release. *Plant, Cell & Environment* **42**: 1630–1644.

Behmanesh M, Sakumi K, Abolhassani N, Toyokuni S, Oka S, Ohnishi YN, Tsuchimoto D, Nakabeppu Y. 2009. ITPase-deficient mice show growth retardation and die before weaning. *Cell Death and Differentiation* **16**: 1315–1322.

Bennett BD, Kimball EH, Gao M, Osterhout R, Van Dien SJ, Rabinowitz JD. 2009. Absolute metabolite concentrations and implied enzyme active site occupancy in *Escherichia coli*. *Nature Chemical Biology* **5**: 593–599.

Bolte S, Cordelieres FP. 2006. A guided tour into subcellular colocalization analysis in light microscopy. *Journal of Microscopy* **224**: 213–232.

Braun H-P. 2020. The oxidative phosphorylation system of the mitochondria in plants. *Mitochondrion* **53**: 66–75.

Budke B, Kuzminov A. 2006. Hypoxanthine incorporation is nonmutagenic in *Escherichia coli*. *Journal of Bacteriology* **188**: 6553–6560.

Budke B, Kuzminov A. 2010. Production of clastogenic DNA precursors by the nucleotide metabolism in *Escherichia coli*. *Molecular Microbiology* **75**: 230–245.

Burgis NE, Brucker JJ, Cunningham RP. 2003. Repair system for noncanonical purines in *Escherichia coli*. *Journal of Bacteriology* **185**: 3101–3110.

Burton K, White H, Sleep J. 2005. Kinetics of muscle contraction and actomyosin NTP hydrolysis from rabbit using a series of metal-nucleotide substrates. *The Journal of Physiology* **563**: 689–711.

Cadet J, Wagner JR. 2013. DNA base damage by reactive oxygen species, oxidizing agents, and UV radiation. *Perspectives in Biology* **5**: a012559.

Cao Y, Tanaka K, Nguyen CT, Stacey G. 2014. Extracellular ATP is a central signaling molecule in plant stress responses. *Current Opinion in Plant Biology* **20**: 82–87.

Carnelli A, Michelis MI, Rasi-Caldogno F. 1992. Plasma membrane Ca-ATPase of radish seedlings I. Biochemical characterization using ITP as a substrate. *Plant Physiology* **98**: 1196–1201.

Chen M, Urs MJ, Sánchez-González I, Olayioye MA, Herde M, Witte C-P. 2018. m^6A RNA degradation products are catabolized by an evolutionarily conserved N^6-methyl-AMP deaminase in plant and mammalian cells. *Plant Cell* **30**: 1511–1522.

Chen M, Witte C-P. 2020. A kinase and a glycosylase catabolize pseudouridine in the peroxisome to prevent toxic pseudouridine monophosphate accumulation. *Plant Cell* **32**: 722–739.

Cho U-H, Seo N-H. 2005. Oxidative stress in *Arabidopsis thaliana* exposed to cadmium is due to hydrogen peroxide accumulation. *Plant Science* **168**: 113–120.

Clyman J, Cunningham RP. 1987. *Escherichia coli* K-12 mutants in which viability is dependent on recA function. *Journal of Bacteriology* **169**: 4203–4210.

Corpas FJ, Leterrier M, Valderrama R, Airaki M, Chaki M, Palma JM, Barroso JB. 2011. Nitric oxide imbalance provokes a nitrosative response in plants under abiotic stress. *Plant Science* **181**: 604–611.

Crécy-Lagard V, Haas D, Hanson AD. 2018. Newly-discovered enzymes that function in metabolite damage-control. *Current Opinion in Chemical Biology* **47**: 101–108.

Dahncke K, Witte C-P. 2013. Plant purine nucleoside catabolism employs a guanosine deaminase required for the generation of xanthosine in Arabidopsis. *Plant Cell* **25**: 4101–4109.

Davies O, Mendes P, Smallbone K, Malys N. 2012. Characterisation of multiple substrate-specific (d)ITP/(d)XTPase and modelling of deaminated purine nucleotide metabolism. *BMB Reports* **45**: 259–264.

Demidchik V. 2015. Mechanisms of oxidative stress in plants: from classical chemistry to cell biology. *Environmental and Experimental Botany* **109**: 212–228.

DeVito S, Woodrick J, Song L, Roy R. 2017. Mutagenic potential of hypoxanthine in live human cells. *Mutation Research* **803–805**: 9–16.

Di Sanità TL, Gabbrielli R. 1999. Response to cadmium in higher plants. *Environmental and Experimental Botany* **41**: 105–130.

Dobrzanska M, Szurmak B, Wyslouch-Cieszynska A, Kraszewska E. 2002. Cloning and characterization of the first member of the Nudix family from *Arabidopsis thaliana*. *Journal of Biological Chemistry* **277**: 50482–50486.

Dubois E, Córdoba-Cañero D, Massot S, Siaud N, Gakière B, Domenichini S, Guérard F, Roldan-Arjona T, Doutriaux M-P. 2011. Homologous recombination is stimulated by a decrease in dUTPase in Arabidopsis. *PLoS ONE* **6**: e18658.

Endo M, Kim JI, Shioi NA, Iwai S, Kuraoka I. 2021. *Arabidopsis thaliana* endonuclease V is a ribonuclease specific for inosine-containing single-stranded RNA. *Open Biology* **11**: 210148.

Fernández-Bautista N, Domínguez-Núñez JA, Moreno MMC, Berrocal-Lobo M. 2016. Plant tissue trypan blue staining during phytopathogen infection. *Bio-Protocol* **6**: e2078.

Fraser JH, Meyers H, Henderson JF, Brox LW, McCoy EE. 1975. Individual variation in inosine triphosphate accumulation in human erythrocytes. *Clinical Biochemistry* **8**: 353–364.

Frederico LA, Kunkel TA, Shaw BR. 1990. A sensitive genetic assay for the detection of cytosine deamination: determination of rate constants and the activation energy. *Biochemistry* **29**: 2532–2537.

Gall AD, Gall A, Moore AC, Aune MK, Heid S, Mori A, Burgis NE. 2013. Analysis of human ITPase nucleobase specificity by site-directed mutagenesis. *Biochimie* **95**: 1711–1721.

Galperin MY, Moroz OV, Wilson KS, Murzin AG. 2006. House cleaning, a part of good housekeeping. *Molecular Microbiology* **59**: 5–19.

Hadwiger LA, Tanaka K. 2017. Non-host resistance: DNA damage is associated with SA signaling for induction of PR genes and contributes to the growth suppression of a pea pathogen on pea endocarp tissue. *Frontiers in Plant Science* **8**: 446.

Haferkamp I, Fernie AR, Neuhaus HE. 2011. Adenine nucleotide transport in plants: much more than a mitochondrial issue. *Trends in Plant Science* **16**: 507–515.

Handley MT, Reddy K, Wills J, Rosser E, Kamath A, Halachev M, Falkous G, Williams D, Cox P, Meynert A *et al.* 2019. ITPase deficiency causes a Martsolf-like syndrome with a lethal infantile dilated cardiomyopathy. *PLoS Genetics* **15**: e1007605.

Hanson AD, Henry CS, Fiehn O, Crécy-Lagard V. 2016. Metabolite damage and metabolite damage control in plants. *Annual Review of Plant Biology* **67**: 131–152.

Harris C, Baulcombe D. 2015. Chlorophyll content assay to quantify the level of necrosis induced by different R gene/elicitor combinations after transient expression. *Bio-Protocol* **5**: e1670.

Heinemann KJ, Yang S-Y, Straube H, Medina-Escobar N, Varbanova-Herde M, Herde M, Rhee S, Witte C-P. 2021. Initiation of cytosolic plant purine nucleotide catabolism involves a monospecific xanthosine monophosphate phosphatase. *Nature Communications* **12**: 6846.

Holmes SL, Turner BM, Hirschhorn K. 1979. Human inosine triphosphatase: catalytic properties and population studies. *Clinica Chimica Acta* **97**: 143–153.

Hooper CM, Castleden IR, Tanz SK, Aryamanesh N, Millar AH. 2017. SUBA4: the interactive data analysis centre for Arabidopsis subcellular protein locations. *Nucleic Acids Research* **45**: D1064–D1074.

James AM, Seal SE, Bailey AM, Foster GD. 2021. Viral inosine triphosphate: a mysterious enzyme with typical activity, but an atypical function. *Molecular Plant Pathology* **22**: 382–389.

Janků M, Luhová L, Petřivalský M. 2019. On the origin and fate of reactive oxygen species in plant cell compartments. *Antioxidants* **8**: 105.

Ji D, Stepchenkova EI, Cui J, Menezes MR, Pavlov YI, Kool ET. 2017. Measuring deaminated nucleotide surveillance enzyme ITPA activity with an ATP-releasing nucleotide chimera. *Nucleic Acids Research* **45**: 11515–11524.

Jiang H-P, Xiong J, Liu F-L, Ma C-J, Tang X-L, Yuan B-F, Feng Y-Q. 2018. Modified nucleoside triphosphates exist in mammals. *Chemical Science* **9**: 4160–4167.

Kamiya H. 2003. Mutagenic potentials of damaged nucleic acids produced by reactive oxygen/nitrogen species: approaches using synthetic oligonucleotides and nucleotides: survey and summary. *Nucleic Acids Research* **31**: 517–531.

Karren P, Lindahl T. 1980. Hypoxanthine in deoxyribonucleic acid: generation by heat-induced hydrolysis of adenine residues and release in free form by a deoxyribonucleic acid glycosylase from calf thymus. *Biochemistry* **19**: 6005–6011.

Keya CA, Crozier A, Ashihara H. 2003. Inhibition of caffeine biosynthesis in tea (*Camellia sinensis*) and coffee (*Coffea arabica*) plants by ribavirin. *FEBS Letters* **554**: 473–477.

Klinker JF, Seifert R. 1997. Functionally nonequivalent interactions of guanosine 5′-triphosphate, inosine 5′-triphosphate, and xanthosine 5′-triphosphate with the retinal G-protein, transducin, and with Gi-proteins in HL-60 leukemia cell membranes. *Biochemical Pharmacology* **54**: 551–562.

Kong RPW, Siu SO, Lee SSM, Lo C, Chu IK. 2011. Development of online high-/low-pH reversed-phase-reversed-phase two-dimensional liquid chromatography for shotgun proteomics: a reversed-phase-strong cation exchange-reversed-phase approach. *Journal of Chromatography A* **1218**: 3681–3688.

Lange PR, Geserick C, Tischendorf G, Zrenner R. 2008. Functions of chloroplastic adenylate kinases in Arabidopsis. *Plant Physiology* **146**: 492–504.

Lerma-Ortiz C, Jeffryes JG, Cooper AJL, Niehaus TD, Thamm AMK, Frelin O, Aunins T, Fiehn O, Crécy-Lagard V, Henry CS *et al.* 2016. 'Nothing of chemistry disappears in biology': the top 30 damage-prone endogenous metabolites. *Biochemical Society Transactions* **44**: 961–971.

Li Z, Kim JH, Kim J, Lyu JI, Zhang Y, Guo H, Nam HG, Woo HR. 2020. ATM suppresses leaf senescence triggered by DNA double-strand break through epigenetic control of senescence-associated genes in Arabidopsis. *New Phytologist* **227**: 473–484.

Lin A-J, Zhang X-H, Chen M-M, Cao Q. 2007. Oxidative stress and DNA damages induced by cadmium accumulation. *Journal of Environmental Sciences* **19**: 596–602.

Lin S, McLennan AG, Ying K, Wang Z, Gu S, Jin H, Wu C, Liu W, Yuan Y, Tang R *et al.* 2001. Cloning, expression, and characterization of a human INOSINE TRIPHOSPHATE PYROPHOSPHATASE encoded by the *itpa* gene. *Journal of Biological Chemistry* **276**: 18695–18701.

Lindahl T. 1993. Instability and decay of the primary structure of DNA. *Nature* **362**: 709–715.

Lindahl T, Nyberg B. 1974. Heat-induced deamination of cytosine residues in deoxyribonucleic acid. *Biochemistry* **13**: 3405–3410.

Linster CL, Van Schaftingen E, Hanson AD. 2013. Metabolite damage and its repair or pre-emption. *Nature Chemical Biology* **9**: 72–80.

Littlejohn GR, Gouveia JD, Edner C, Smirnoff N, Love J. 2010. Perfluorodecalin enhances in vivo confocal microscopy resolution of *Arabidopsis thaliana* mesophyll. *New Phytologist* **186**: 1018–1025.

Liu S, Yu F, Yang Z, Wang T, Xiong H, Chang C, Yu W, Li N. 2018. Establishment of dimethyl labeling-based quantitative acetylproteomics in Arabidopsis. *Molecular & Cellular Proteomics* **17**: 1010–1027.

Muraoka M, Fukuzawa H, Nishida A, Okano K, Tsuchihara T, Shimoda A, Suzuki Y, Sato M, Osumi M, Sakai H. 1999. The effects of various GTP analogues on microtubule assembly. *Cell Structure and Function* **24**: 101–109.

Nagy GN, Leveles I, Vértessy BG. 2014. Preventive DNA repair by sanitizing the cellular (deoxy)nucleoside triphosphate pool. *The FEBS Journal* **281**: 4207–4223.

Niehaus M, Straube H, Künzler P, Rugen N, Hegermann J, Giavalisco P, Eubel H, Witte C-P, Herde M. 2020. Rapid affinity purification of tagged plant mitochondria (Mito-AP) for metabolome and proteome analyses. *Plant Physiology* **182**: 1194–1210.

Niehaus M, Straube H, Specht A, Baccolini C, Witte C-P, Herde M. 2022. The nucleotide metabolome of germinating *Arabidopsis thaliana* seeds reveals a central role for thymidine phosphorylation in chloroplast development. *Plant Cell* **34**: 3790–3813.

Niehaus TD, Patterson JA, Alexander DC, Folz JS, Pyc M, MacTavish BS, Bruner SD, Mullen RT, Fiehn O, Hanson AD. 2019. The metabolite repair enzyme NIT1 is a dual-targeted amidase that disposes of damaged glutathione in Arabidopsis. *The Biochemical Journal* **476**: 683–697.

Niehaus TD, Richardson LGL, Gidda SK, ElBadawi-Sidhu M, Meissen JK, Mullen RT, Fiehn O, Hanson AD. 2014. Plants utilize a highly conserved system for repair of NADH and NADPH hydrates. *Plant Physiology* **165**: 52–61.

Noskov VN, Staak K, Shcherbakova PV, Kozmin SG, Negishi K, Ono B-C, Hayatsu H, Pavlov YI. 1996. *HAM1*, the gene controlling 6-N-hydroxylaminopurine sensitivity and mutagenesis in the yeast *Saccharomyces cerevisiae*. *Yeast* **12**: 17–29.

Oberacker P, Stepper P, Bond DM, Höhn S, Focken J, Meyer V, Schelle L, Sugrue VJ, Jeunen G-J, Moser T *et al.* 2019. Bio-On-Magnetic-Beads (BOMB): open platform for high-throughput nucleic acid extraction and manipulation. *PLoS Biology* **17**: e3000107.

Osheroff N, Shelton ER, Brutlag DL. 1983. DNA TOPOISOMERASE II from *Drosophila melanogaster*. Relaxation of supercoiled DNA. *Journal of Biological Chemistry* **258**: 9536–9543.

Pang B, McFaline JL, Burgis NE, Dong M, Taghizadeh K, Sullivan MR, Elmquist CE, Cunningham RP, Dedon PC. 2012. Defects in purine nucleotide metabolism lead to substantial incorporation of xanthine and hypoxanthine into DNA and RNA. *Proceedings of the National Academy of Sciences, USA* **109**: 2319–2324.

Pavlov II. 1986. Mutants of *Saccharomyces cerevisiae* supersensitive to the mutagenic effect of 6-N-hydroxylaminopurine. *Genetika* **22**: 2235–2243.

Rampazzo C, Miazzi C, Franzolin E, Pontarin G, Ferraro P, Frangini M, Reichard P, Bianchi V. 2010. Regulation by degradation, a cellular defense against deoxyribonucleotide pool imbalances. *Mutation Research* **703**: 2–10.

Rinne J, Witte C-P, Herde M. 2021. Loss of MAR1 Function is a marker for co-selection of CRISPR-induced mutations in plants. *Frontiers in Genome Editing* **3**: 723384.

Rudd SG, Valerie NCK, Helleday T. 2016. Pathways controlling dNTP pools to maintain genome stability. *DNA Repair* **44**: 193–204.

Sakumi K, Abolhassani N, Behmanesh M, Iyama T, Tsuchimoto D, Nakabeppu Y. 2010. ITPA protein, an enzyme that eliminates deaminated purine nucleoside triphosphates in cells. *Mutation Research* **703**: 43–50.

Savchenko A, Proudfoot M, Skarina T, Singer A, Litvinova O, Sanishvili R, Brown G, Chirgadze N, Yakunin AF. 2007. Molecular basis of the antimutagenic activity of the house-cleaning inosine triphosphate pyrophosphatase RdgB from *Escherichia coli*. *Journal of Molecular Biology* **374**: 1091–1103.

Schroader JH, Jones LA, Meng R, Shorrock HK, Richardson JI, Shaughnessy SM, Lin Q, Begley TJ, Berglund JA, Fuchs G *et al.* 2022. Disease-associated inosine misincorporation into RNA hinders translation. *Nucleic Acids Research* **50**: 9306–9318.

Simone PD, Pavlov YI, Borgstahl GEO. 2013. ITPA (inosine triphosphate pyrophosphatase): from surveillance of nucleotide pools to human disease and pharmacogenetics. *Mutation Research* **753**: 131–146.

Spee JH, Vos WM, Kuipers OP. 1993. Efficient random mutagenesis method with adjustable mutation frequency by use of PCR and dITP. *Nucleic Acids Research* **21**: 777–778.

Stenmark P, Kursula P, Flodin S, Gräslund S, Landry R, Nordlund P, Schüler H. 2007. Crystal structure of human inosine triphosphatase. Substrate binding and implication of the inosine triphosphatase deficiency mutation P32T. *Journal of Biological Chemistry* **282**: 3182–3187.

Straube H, Herde M. 2022. Purification and analysis of nucleotides and nucleosides from plants. In: Ayyar BV, Arora S, eds. *Affinity chromatography. Methods in molecular biology, vol. 2466*. New York, NY: Humana, 145–155.

Straube H, Niehaus M, Zwittian S, Witte C-P, Herde M. 2021. Enhanced nucleotide analysis enables the quantification of deoxynucleotides in plants and algae revealing connections between nucleoside and deoxynucleoside metabolism. *Plant Cell* **33**: 270–289.

Thomas MJ, Platas AA, Hawley DK. 1998. Transcriptional fidelity and proofreading by RNA POLYMERASE II. *Cell* **93**: 627–637.

Tomlinson KR, Pablo-Rodriguez JL, Bunawan H, Nanyiti S, Green P, Miller J, Alicai T, Seal SE, Bailey AM, Foster GD. 2019. *Cassava brown streak virus* HAM1 protein hydrolyses mutagenic nucleotides and is a necrosis determinant. *Molecular Plant Pathology* **20**: 1080–1092.

Traube FR, Schiffers S, Iwan K, Kellner S, Spada F, Müller M, Carell T. 2019. Isotope-dilution mass spectrometry for exact quantification of noncanonical DNA nucleosides. *Nature Protocols* **14**: 283–312.

Tripathi D, Nam A, Oldenburg DJ, Bendich AJ. 2020. Reactive oxygen species, antioxidant agents, and DNA damage in developing maize mitochondria and plastids. *Frontiers in Plant Science* **11**: 596.

Valderrama R, Corpas FJ, Carreras A, Fernández-Ocaña A, Chaki M, Luque F, Gómez-Rodríguez MV, Colmenero-Varea P, Del Río LA, Barroso JB. 2007. Nitrosative stress in plants. *FEBS Letters* **581**: 453–461.

Valli AA, López RG, Ribaya M, Martínez FJ, Gómez DG, Garcia B, Gonzalo I, de Prádena AG, Pasin F, Montanuy I *et al.* 2022. Maf/ham1-like pyrophosphatases of non-canonical nucleotides are host-specific partners of viral RNA-dependent RNA polymerases. *PLoS Pathogens* **18**: e1010332.

Vanderheiden BS. 1979. Possible implication of an inosinetriphosphate metabolic error and glutamic acid decarboxylase in paranoid schizophrenia. *Biochemical Medicine* **21**: 22–32.

Vidal AE, Yagüe-Capilla M, Martínez-Arribas B, García-Caballero D, Ruiz-Pérez LM, González-Pacanowska D. 2022. Inosine triphosphate pyrophosphatase from *Trypanosoma brucei* cleanses cytosolic pools from deaminated nucleotides. *Scientific Reports* **12**: 6408.

Wang C, Liu Z. 2006. Arabidopsis ribonucleotide reductases are critical for cell cycle progression, DNA damage repair, and plant development. *Plant Cell* **18**: 350–365.

Weber J, Senior AE. 2001. Bi-site catalysis in F1-ATPase: does it exist? *Journal of Biological Chemistry* **276**: 35422–35428.

Werner AK, Sparkes IA, Romeis T, Witte C-P. 2008. Identification, biochemical characterization, and subcellular localization of Allantoate amidohydrolases from Arabidopsis and soybean. *Plant Physiology* **146**: 418–430.

Winter D, Vinegar B, Nahal H, Ammar R, Wilson GV, Provart NJ. 2007. An "Electronic Fluorescent Pictograph" browser for exploring and analyzing large-scale biological data sets. *PLoS ONE* **2**: e718.

Witte C-P, Herde M. 2020. Nucleotide metabolism in plants. *Plant Physiology* **182**: 63–78.

Witte C-P, Rosso MG, Romeis T. 2005. Identification of three urease accessory proteins that are required for urease activation in Arabidopsis. *Plant Physiology* **139**: 1155–1162.

Yan S, Wang W, Marqués J, Mohan R, Saleh A, Durrant WE, Song J, Dong X. 2013. Salicylic acid activates DNA damage responses to potentiate plant immunity. *Molecular Cell* **52**: 602–610.

Yang Z-B, He C, Ma Y, Herde M, Ding Z. 2017. Jasmonic acid enhances Al-induced root growth inhibition. *Plant Physiology* **173**: 1420–1433.

Yoneshima Y, Abolhassani N, Iyama T, Sakumi K, Shiomi N, Mori M, Shiomi T, Noda T, Tsuchimoto D, Nakabeppu Y. 2016. Deoxyinosine triphosphate induces MLH1/PMS2- and p53-dependent cell growth arrest and DNA instability in mammalian cells. *Scientific Reports* **6**: 32849.

Yoshimura K, Ogawa T, Ueda Y, Shigeoka S. 2007. *ATNUDX1*, an 8-oxo-7,8-dihydro-2′-deoxyguanosine 5′-triphosphate pyrophosphohydrolase, is responsible for eliminating oxidized nucleotides in *Arabidopsis*. *Plant & Cell Physiology* **48**: 1438–1449.

Supporting Information

Additional Supporting Information may be found online in the Supporting Information section at the end of the article.

Fig. S1 Comparative sequence analysis of inosine triphosphate pyrophosphatases from several phylogenetically distant model organisms of all kingdoms of life.

Fig. S2 Comparative sequence analysis of inosine triphosphate pyrophosphatases.

Fig. S3 Phenotyping of wild-type and *itpa* mutant plants.

Fig. S4 Characterization of *itpa* mutant and overexpressor lines.

Fig. S5 Chromatograms of inosine triphosphate and inosine diphosphate analyzed by hypercarb chromatography.

Fig. S6 Relative concentration of different nucleotides in rosette leaves of 35-d-old wild-type and itpa mutant plants.

Fig. S7 Manipulation of inosine monophosphate content in leaves of *Nicotiana benthamiana* alters the concentration of guanosine monophosphate and xanthosine monophosphate, but not inosine triphosphate and guanosine triphosphate.

Fig. S8 Concentration of inosine in isolated RNA of wild-type and *itpa-1* plants.

Fig. S9 Loss-of-function of inosine triphosphate pyrophosphatase leads to differential upregulation of transcripts associated with GO terms of biological processes, molecular functions, and cellular components.

Methods S1 Supporting Methods.

Table S1 List of primers used in this study.

Table S2 List of differentially expressed genes.

Table S3 List of the GO term enrichment analysis.

Table S4 Raw and statistical data.

Table S5 Substrates tested for biochemical activity with inosine triphosphate pyrophosphatase.

Table S6 Ratios (deoxy)inosine per million molecules (deoxy) adenosine in DNA and RNA, respectively.

Please note: Wiley is not responsible for the content or functionality of any Supporting Information supplied by the authors. Any queries (other than missing material) should be directed to the *New Phytologist* Central Office.